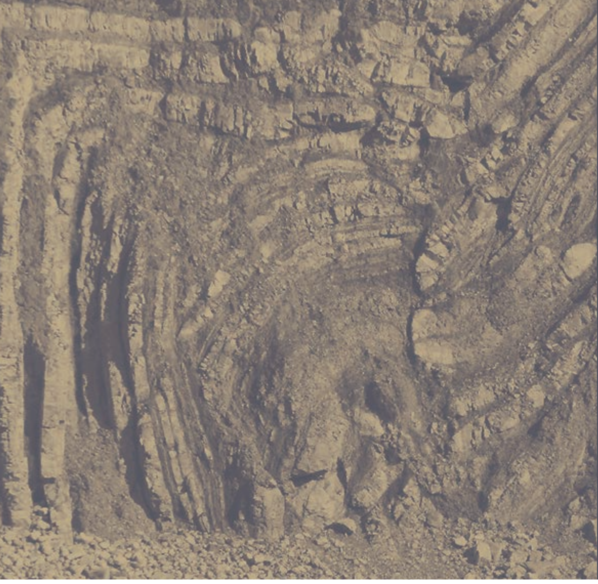

SARES 2019

SOUTH AFRICAN ROCK ENGINEERING SYMPOSIUM

A COLLAGE OF SOUTH AFRICAN ROCK ENGINEERING

26 JUNE 2019

MISTY HILLS COUNTRY HOTEL & CONFERENCE CENTRE,
MULDERSDRIFT, GAUTENG

SANIRE
SOUTH AFRICAN NATIONAL INSTITUTE
OF ROCK ENGINEERING

Foreword

The South African National Institute of Rock Engineering (SANIRE) and the Southern African Institute of Mining and Metallurgy (SAIMM) take great pleasure in introducing the proceedings of the South African Rock Engineering Symposium (SARES 2019) held at the Misty Hills Conference Centre, Muldersdrift, Johannesburg on 26 June 2019.

Across South Africa, many different minerals and metals are mined using a range of unique mining methods and machinery. South African mines differ greatly in depth, layouts and geometries. During the past centuries, mining in South Africa ranged from the early alluvial diamond mining in the Cape to deep level gold mining in the central and northern part of the country. South Africa's mining methods have evolved during the past decades, making many innovative advances in mechanisation and improved support efficiencies. High stress mining in the world's deepest gold mine as well as the world's deepest platinum mine, has extended the boundaries of rock engineering and mine design.

Of the 6 papers included in the proceedings, 5 are from South Africa, and 1 from Italy.

The Symposium was jointly organized by the South African National Institute of Rock Engineering (SANIRE) and the Southern African Institute of Mining and Metallurgy (SAIMM).

We are grateful to the presenters and delegates for taking time out of their busy schedules to come and share their knowledge and expertise. The sponsors are also thanked for their generous contributions to making this event possible. Thanks is also due to the organizing committee and technical reviewers. As always, we are grateful for the dedication and the organizational skills of the SAIMM secretariat.

Paul Couto
Editor

Committee Members

P. Couto and J. Maritz

Contents

Traditional core logging revolutionised

B. Klaas[1], N. Khanyile[2], and M.F. Phamotse[3]

[1]Knight Piésold, South Africa
[2]MSKC JV/ Aurecon, South Africa
[3]MSKC JV/ LHDA, Lesotho

In this digital age, processes need to become more innovative for reasons of efficiency. Traditional core logging is laborious and time consuming, both in the field and office.

StereoCore™ PhotoLog, is a photogrammetric software package that enables paperless, rig-side, digital data acquisition while the core is fresh, ensuring vital information is not lost during transportation and reducing hours of data capture in the office. Colour coded data markers tag all features on undistorted images, after which the tasks of depth registering the core, depth referencing the tags, and measuring structure alpha and beta angles can be done remotely. The annotated images enable unambiguous real-time quality control as well as thorough quality assessment audits, thereby ensuring full data integrity. All the on-site and review phase checks show that accurate data is being captured and reliable outputs calculated by StereoCore™.

StereoCore™ was successfully implemented in the Lesotho Highlands Water Project Phase II investigations.

PROJECT BACKGROUND AND INTRODUCTION

The Lesotho Highlands Water Commission (LHWC) represents and advises the two governments and has an overall responsibility and oversight function for the Lesotho Highlands Water Project (LHWP) which is a project between the Kingdom of Lesotho and the Republic of South Africa. The Lesotho Highlands Development Authority (LHDA) is the implementing authority on behalf of the two Governments. The Trans-Caledon Tunnelling Authority (TCTA) in South Africa is responsible for operations and maintenance of LHWP infrastructure in South Africa.

Phase II of the LHWP is currently under construction, with the scheme expected to ultimately transfer some 70 m^3/s of water to Gauteng in South Africa, and using the water transfer system to generate electricity for Lesotho.

Phase I (1A and 1B spanning 1986 to 2003) of the LHWP comprised:

- Katse Dam and the Transfer Tunnel from Katse to Muela Hydropower Station,
- Muela Hydropower Station, Muela Dam, and the delivery tunnel from Muela Dam to the Ash River Outfall in South Africa.
- Mohale Dam, and the Mohale Tunnel transferring water from the Mohale Reservoir to Katse Reservoir.
- Matsoku Diversion Weir and tunnel transferring water to Katse Reservoir from the adjacent Matsoku Valley.

Phase II of the LHWP is being implemented in terms of two distinct components: a water delivery system to augment the delivery of water to South Africa and a hydropower generation system, which will increase the current electricity generation capacity in Lesotho.

The water transfer component of Phase II of the LHWP commenced with a feasibility study in 2005 and comprises the design and construction of Polihali Dam and Polihali Transfer Tunnel (PTT). The dam is envisaged to be a 163,5m high concrete-faced rockfill dam situated downstream of the confluence of the Senqu (Orange/Gariep) and Khubelu Rivers. The PTT will be ~38km long and will transfer water from Polihali Reservoir to Katse Dam.

Metsi, a Senqu-Khubelu Consultants Joint Venture (MSKC JV) was appointed by LHDA as part of Phase II of the LHWP, to provide professional services for the design and construction supervision of the Polihali Transfer Tunnel. The authors are part of the MSKC JV geotechnical team and will be referring exclusively to pertinent aspects of the PTT investigations in this paper.

PROJECT REQUIREMENTS

The LHWP developed a project specific logging standard which was formulated between 1985 and 1987 by John Ager and Richard Galliers while working for Lahmeyer MacDonald Consortium and Olivier Shand Consortium respectively. This logging standard required large amounts of data to be captured during the geotechnical investigations. The data comprised drilling records, in situ testing, rock fabric, discontinuity data, rock strength, weathering, recoveries, general descriptions, comments on rock durability and additional comments during core logging. These parameters were recorded manually as 31 individual data entries – a time consuming task.

Thirty-four years later, technology has advanced along with the need for data capture to be more efficient while maintaining the established logging standard. Strict timelines applied to this project and the MSKC JV geotechnical team was under constant pressure to deliver quality data that can be compared to the vast amounts of legacy data from earlier phases of the LHWP. Hence the challenge to skew the graph of time by enhancing the amount and quality of data collected, while reducing the time spent capturing it. With the pressures and constraints mentioned above, MSKC JV explored new technologies to provide the requisite efficiency.

CONVENTIONAL LOGGING AND MAKING THE SHIFT

The prescribed South African logging standard published by Brink and Bruin (2002), recommends that logging commences with the calculation of core recoveries and losses, rock quality designation (RQD) and fracture frequency using a measuring tape. The core recoveries are calculated per drill run. The RQD is a measure of the quality of the rock mass, and is measured by the addition of core pieces over 100 mm in length, divided by the length of the core run and is expressed as a percentage. The fracture frequency is the measure of all natural breaks and is commonly measured at metre intervals.

Upon completion of these measurements, the rock is described according to the prescribed logging standard and discontinuities are characterised. Discontinuity characterisation includes the use of rudimentary tools such as the protractor, goniometer and/or beta-strip to calculate the alpha and beta angles. Alpha angles are measured at every joint as the acute angle between the core axis and the long axis of the intersection ellipse of the joint which is associated with the dip of the joint plane. The beta angle is measured on orientated core with respect to the reference line to provide orientation (dip direction) of the joint planes. These measurements are often rigorous and time consuming.

Traditionally, a log sheet is used on site to record the required data and rock parameters. The information is later typed out at the office and transferred into a preferred computer programme to generate a paper log. The paper log is typically reviewed by a senior engineering geologist or geotechnical engineer and often there is a need for the reviewer to travel to site or core shed to ensure the accuracy of the logged data. This increases the cost of the investigation due to additional travel time and costs.

StereoCore™, is able to accurately calculate the core recoveries, rock quality designation metres (RQDm), fracture count for fracture frequency and the alpha and beta angles, thereby significantly reducing the logging time on site. The logging is conducted on a digital photograph allowing the reviewer to remotely conduct the detailed quality assessments, also reducing travel and site accommodation costs.

STEREOCORE™ WITH ITS USER DEFINABLE CAPABILITIES

StereoCore™ PhotoLog is a photogrammetric software package that enables paperless, rig-side, digital data acquisition which reduces hours of data capture in-office. The programme has been applied to mining projects and now, for the first time, successfully implemented on a major geotechnical project in Africa, the Lesotho Highlands Water Project.

StereoCore™ rapidly captures large amounts of logging parameters with ease while the core is fresh and pristine, ensuring vital information is not lost during transportation and/or storage. StereoCore™ allows the task of depth registering the core, depth referencing the logged data and finding the alpha and beta angles for structures to be done remotely to deliver the logs in the shortest time possible.

TYPICAL WORK FLOW

The typical work flow on a StereoCore™ core logging programme encompasses five basic steps, as illustrated in Figure 1 below.

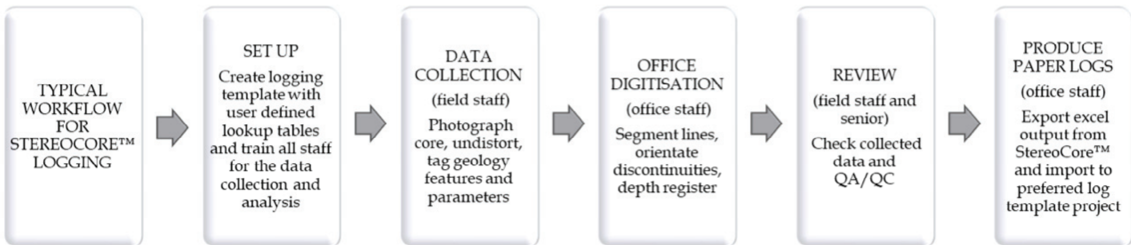

Figure 1. Typical work flow

Setup:
Before the project can commence with the data collection, a log format editor is used to setup the customised template that will be populated during logging/ data acquisition. The log format template may be adjusted throughout the project as needed and to enable additional capture of data which may have initially been excluded when setting up the template. The StereoCore™ programme runs on a Microsoft Windows operating system. Typically, tablets were used to collect data in the field and the analysis transferred and continued to a laptop.

Data collection:
Photographs are taken by either placing the core trays on a customized reference frame for orientated boreholes, or simply using the inside dimensions of the core box to calibrate photographs of core from unoriented boreholes. These photographs are then uploaded into StereoCore™ and the programme digitally undistorts the photographs to provide a 3D image; this allows depth registered tagging of the core for logging purposes. Colour-coded data markers (discontinuity structures, rock descriptions and

other salient features) are placed directly onto the undistorted photograph to tag different features of the core as shown in Figure 2.

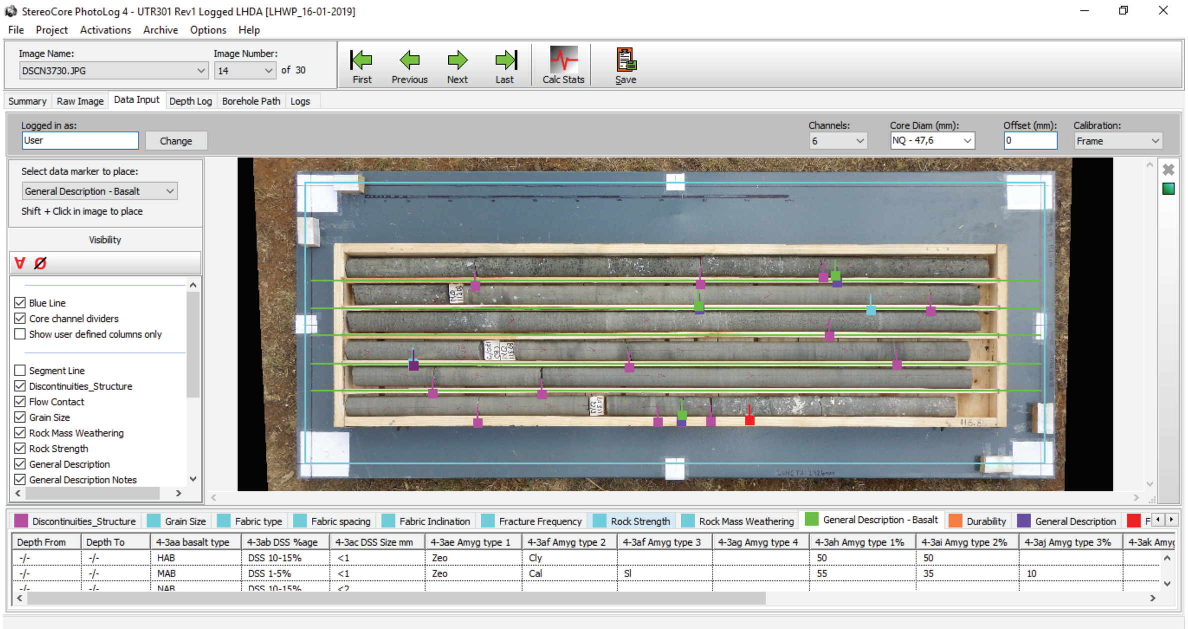

Figure 2. Shows the undistorted core photo marked up using the orientated core frame. The green core channel dividers and colour coded data tags are visible.

Office digitisation

The digitisation process involves depth registration of the core which can be performed remotely to reduce the delivery time while the fieldwork on-site continues. This is carried out by marking the core blocks and assigning their depth using the core block data marker. A segment line is drawn over the axis of each piece of core and denotes whether the core is solid core or matrix/rubble and further indicates the nature of the break (none, natural or mechanical in blue, yellow or red, respectively) at the start of each segment. Oriented core segment lines indicate the location of the reference line of each segment (top blue or bottom red). Unoriented core is marked by a yellow segment line. The segment line callipers should be adjusted to match the visible diameter of the core.

Snapping the data markers onto the segment lines anchors each data marker to its position along the core with a depth reference. Two depths are provided, standard depth referencing where depth is measured from the preceding core block, and stacked depth referencing where depth is automatically adjusted by the StereoCore™ software for core overrun errors.

Usually all the data markers are simultaneously snapped per photo. However, markers can be snapped and re-snapped individually where required.

Planar structures are transformed once snapped to the segment line as a colour coded ellipse fitting the structure to represent the plane through the core thereby providing alpha angles for all data and beta angles when the core has been orientated.

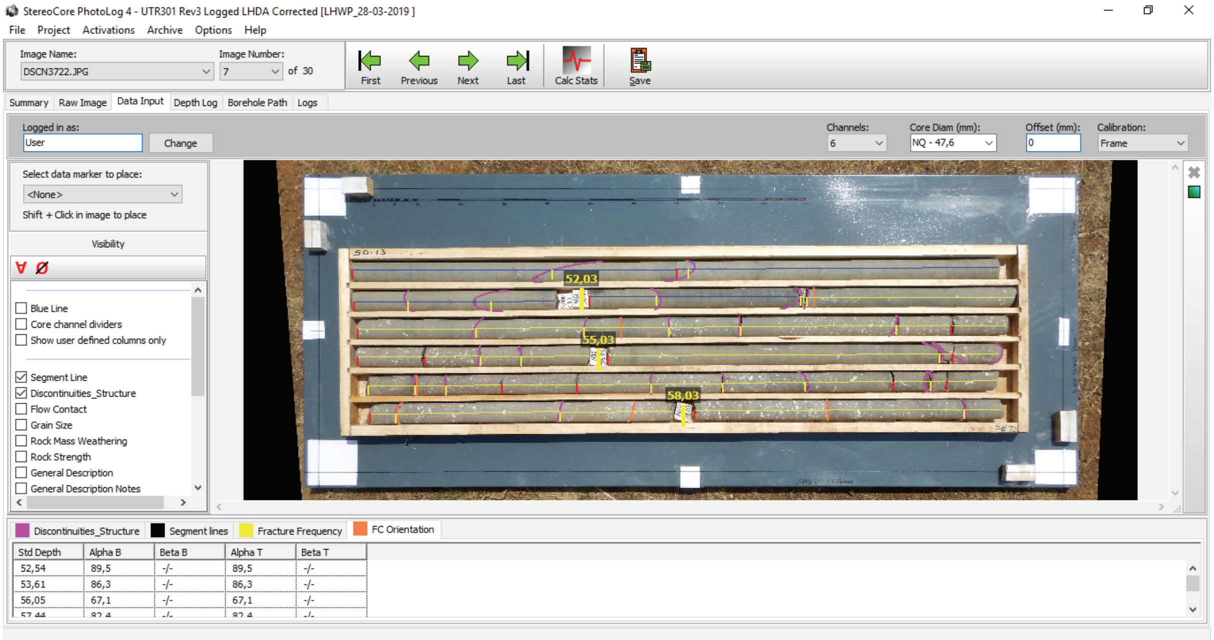

Figure 3. Colour-coded discontinuity/structure data (pink and orange) snapped to segment lines and core blocks as a depth registered image

Review

The review process includes two stages where the initial stage is a review of the office digitisation by the field staff. The data file is returned to the field staff who check that the information is correctly depth registered, snapped and visually shown as observed in the core trays during core logging/ data collection.

The second stage of the review is a detailed quality assessment audit by a senior engineering geologist or geotechnical engineer to ensure full data integrity and unambiguous quality control.

Paper logs

After review, the logging data is exported from StereoCore™ to an Excel workbook or CSV output file ready for integration in a number of core-logging software programmes. The user then chooses the preferred computer software to produce the paper log such as WinLog, dotPlot or gINT. Minor data manipulation may be required to transform the Excel file for the programme of choice. The exported data can be easily edited to fit the master spreadsheet of the log template used. The user may export all the data or select specific data fields to be included in the export. A typical output file contains multiple sheets providing one sheet per data category. StereoCore™ does not output the mechanical log (recoveries) as a percentage-based unit, but rather as recoveries by metre – this is because no industry standard exists as to what the percentages measure; whereas, a recovery stated in terms of metres is unambiguous. A user input is required to transform the recoveries to a percentage for the template. Figure 4 gives an example of a paper log created for this project using StrataExplorer WinLog.

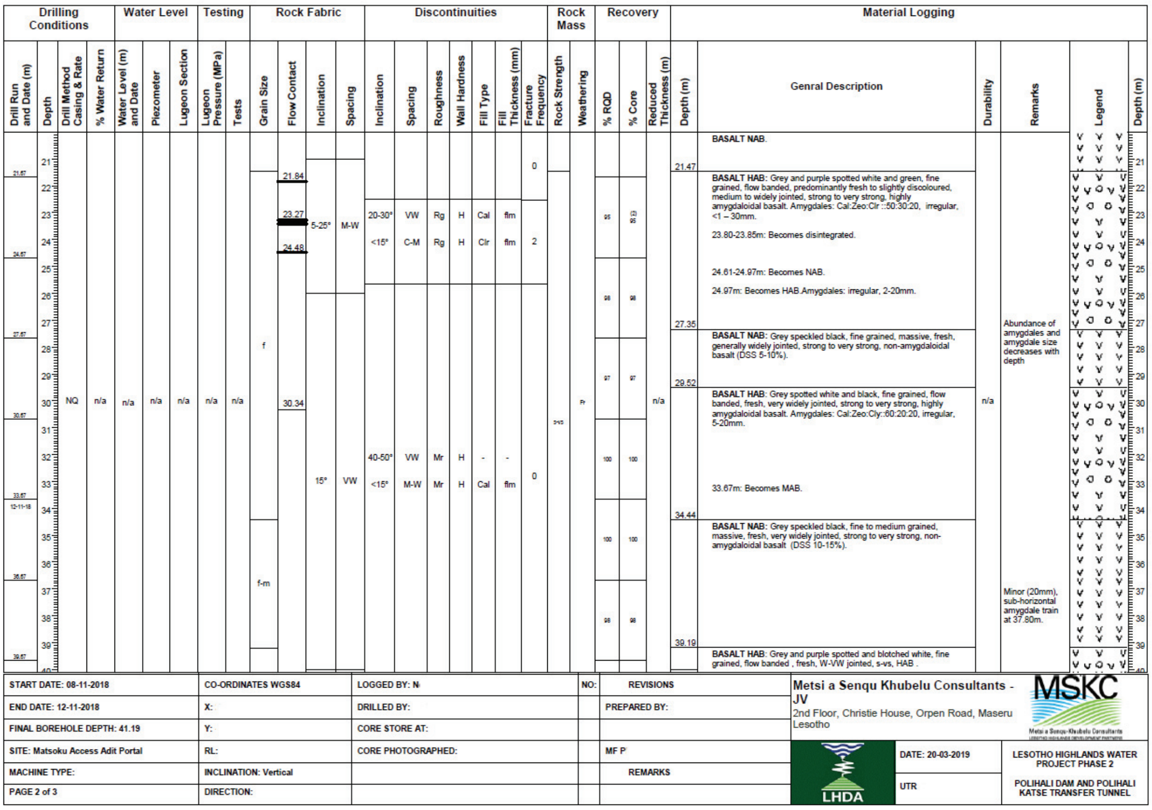

Figure 4. A paper log is produced according to the data to be presented. This is an example of draft log for QA/QC for the project

STEREOCORE™ DATA VERIFICATION

StereoCore™ is run through multiple checks to ensure the programme is capturing and calculating data correctly. The software is periodically bench tested and the results made available to end users. End users are also encouraged to perform their own data checks (for example, by taking their own alpha and beta measurements for a sample of the structures). In addition, the software has been field tested on multiple projects both within South Africa and internationally.

The introduction of new technology may cause doubt regarding the accuracy of data. Multiple checks were carried out by the site and review staff to ensure confident data comparisons can be made with the historical data. On site alpha and beta angles were measured and compared to independently drawn ellipses and StereoCore™ calculated alpha and beta angles. Minor discrepancies were observed in this stage due to the level of precision by the user drawing the ellipse. Care has to be taken to set up the StereoCore™ log format to output the correct alpha and beta values for comparison, as StereoCore™ has the capability to output angles for comparison with several different goniometers that are in common use. In this case beta strips were used for manual measurements and the log format was set up to output the structure angles accordingly.

When recoveries were measured, both on site and review phase, recoveries were compared with StereoCore™ data and the differences were found to be negligible, which could be attributed to inaccuracies measuring on site, or inaccuracies in the drawing of segment lines.

In addition, the integration of the downhole geophysics or borehole scanner logs can be used to QC the depth registration and supplement the logging data.

The StereoCore™ working file and draft logs were instrumental in highlighting areas of concern which became the focus for the review. The marked up draft logs and StereoCore™ working file allowed for immediate correction on site. All the on-site and review phase checks showed that accurate data was being captured and reliable outputs calculated by StereoCore™. Minor discrepancies noted were attributed to human error. When using StereoCore™, it is imperative that the user is diligent in their efforts to minimise these errors.

THE GOOD AND THE BAD: SUMMARY OF NEW TECHNOLOGY FOR CORE LOGGING

In order to reflect on the advantages of using improved technology a pro's and con's list has been generated below. The list summarises the main advantages and disadvantages of using StereoCore™ for core logging in a geotechnical application.

Advantages	**Limitations and Remarks**
StereoCore™ developer assists with free project set up, template creation and staff training	Setup costs - purchasing the tablets and staff training
Support from StereoCore™ to assist, explain or improve any aspect on an on-going basis	The software is licenced on a pay-per-use basis, charging an image processing fee per photo
Software is free to download	Technical failures of hardware equipment on site do occur which could slow or halt the logging process
Staff are easily trained in the new software	Structural features on the underside of the core in the trays are difficult to present on the image, but once depicted quickly warn the user of hidden data
Able to tailor to specific projects and create customised look ups and drop downs	Non-planar features such as the curved *intra-flow* joints and some discontinuities related to *onion skin* weathering, cannot be accurately depicted
Simple reference frame table setup/ drawn on site for orientated core	Direct digital data capture must be properly saved to avoid missing or erroneous data such as *wandering tags* or *jump snaps*
Simple and user-friendly program to speed up rig-side logging	
Logging core rig site and photographed in pristine condition	
More data is collected with ease as input is direct to digital	
Digital option at boreholes or paper logging to be captured later – in case technology fails	
Easy visual analysis and review at any point during investigation	
Increase logging speed due to automatic calculation of the recoveries, RQD and fracture count once depth registered	
Provides alpha and beta angles on orientated core without requiring a goniometer or beta strips and reduces excessive handling of cores which reduces core damage	
Formatting of data is simple and easily manipulated	
Multiple users can add data remotely and later merge the files allowing for collaboration on the same borehole	

StereoCore™ can be used to verify/audit the drilling data as part of QA/QC	
When backed up, irretrievable loss of data is almost impossible in a digital format	
Output to Excel workbook or CSV file	
The program facilitates QC of the ongoing drilling contract	
Undistortion can be carried out multiple times on the same photograph at no extra cost	

The following points are also pertinent in terms of the use of the StereoCore™ system on this project, in comparison to traditional ways of core logging:

- The startup phase included purchasing logging tablets, training of staff and the development of a customised logging template and format lookup tables. This incurred additional time and cost inputs in comparison to the relatively quick startup phase of traditional methods which merely require a pen and paper and using existing field log templates.
- The better the quality of the tablet used on site for data collection, the better the users experience on site during tagging.
- A long-lasting battery source, durable cover/exterior, high contrast and responsive touch screen are highly advantageous for the Windows operating system tablet.

During logging and digitisation of the borehole, special care must be taken as occasionally tags may wander if accidentally moved by mouse clicks and/or finger swipes on the tablet. Furthermore, it remains difficult to graphically present the ellipses of hidden or sub-vertical joints. As with traditional logging, non-planar discontinuities remain a challenge for representation and measurement.

MSKC JV has found great advantage in the pre-set dropdown menu selection during logging when using StereoCore™ and benefits derived from the direct digital data capture. Easy visual analysis and on-site or remote review were also possible at any point during the geotechnical investigations. This audit facility added further value as a quality control on the drilling contract of work done by both the drillers and the field geologists.

In summary, the far-reaching effects and increase in data capture speed when using StereoCore™ is likely to aid projects the larger the data set becomes. It is envisaged that large, multi-borehole and multi-phased projects will benefit the most from the speed of input and analysis capability using this method.

ACKNOWLEDGEMENTS

We would like to thank Lesotho Highlands Development Authority for giving permission to use the data in this article.

We would also like to thank Dr John Orpen and David Orpen, StereoCore™ Developers, for their continued training and support for the duration of this project.

We also thank Gerhard Keyter for his review of this paper.

REFERENCES

Brink, A. B. A. and Bruin, R. M. H. (2002). Guidelines for soil and rock logging in South Africa. Proceedings of the Geoterminology Workshop 1990. Association of Engineering Geologists, South African Institute of Civil Engineering and South African Institute for Engineering Geologists, 2nd Impression.

Lahmeyer MacDonald Consortium / Olivier Shand Consortium (1986). LHWP logging standard, Lesotho Highlands Water Project Feasibility Study, Main Report, Supporting Reports, and Appendices.

MSKC (2018). Earlier Geotechnical Studies & Investigations. MSKC Report No. P2W-3007-RPT-0001 V01.

StereoCore™ PhotoLog 4.7.4 Help Manual, Ground Modelling Technologies Ltd.

Bronwen Klaas

Engineering Geologist
MSKC JV (Knight Piésold)

Bronwen is an engineering geologist working in the field of geotechnical engineering for more than eight years. She is mainly involved in geotechnical investigations that includes fieldwork by logging of test pits, auger holes, rotary cored boreholes and percussion drilled holes. She analyses the data with reference to provide geotechnical recommendations for foundations of structures. She is also involved in numerous investigations for construction material source identification, slope stability evaluation, dolomite stability assessments as well as compact, large and linear developments that includes bridges, pipelines and roads. Bronwen has been involved in the geotechnical investigation of the Lesotho Highlands Water Project: Phase 2 –for the Polihali Transfer Tunnel between September 2018 and May 2019.

Using interferometric radar technology as a complementary instrument to improve safety in underground mines

N. Boldrini [1], M. Rubino[1], M. Rossi [1], M. Cecchetti [1], F. Coppi[1], N. Coli [1], C. Thomson[2], M. Radzilani[2], and D. van Rensburg[3]

[1]GeoRadar, Italy
[2]IDS GeoRadar, South Africa
[3]Geoprime, South Africa

Fall of ground (FOG) continues to be one of the most serious causes of incidents, and underground mine fatalities and damage to machinery are attributed mainly to FOG. As mines grow deeper, it is essential to understand rock mass behaviour under high stress. Critical monitoring is one of the keys to prevent accidents, ensuring a safe workplace for all, and saving time and cutting costs. To respond to this need, IDS GeoRadar (part of Hexagon), a provider of radar technology in the mining industry, developed HYDRA-U, a radar monitoring system able to provide sub-millimetre displacement accuracy at a spatial resolution of tens of centimetres, with updated displacement information every 30 seconds and the capability to warn of impending rock fall. HYDRA-U, a compact and light interferometric radar system, was specifically designed and developed for rock mechanic engineers in underground mining to monitor fall of ground precursors, provide early warning to evacuate people and machinery at risk and enable preliminary risk assessments on potentially exposed instabilities in underground areas.

INTRODUCTION

FOG is one of the most serious causes of incidents: underground mine fatalities and damage to machinery and injuries to workers are attributable mainly to FOG. Also, in highly automated underground mines, where the human presence is reduced to a minimum, ground falls represent a major risk of damage to expensive machinery and interrupting operations. The importance of strata control is fundamental, in particular the control and management of the stability of rocks immediately around excavations.

Although safety is considered one of the key factors, limitations in feasible technological solutions, cost, and the very nature of underground mining, have restricted the development of remote monitoring systems that ensure full safety for the miners with respect to monitoring and prediction of ground collapses. The use of monitoring systems to detect wall movements in surface mining has been recognised as the primary technology for safe working conditions. During the last ten years, the development and optimisation of interferometric radar technology has greatly contributed to the prediction of slope movements and reduction of incidents and fatalities related to slope failures in open-pit mines. The same cannot be said for underground mines, where deformation measurement is still in most cases restricted to contact sensors such as extensometers, strain gauges and fibre optic systems. These can provide pointwise information of some areas, but installation, maintenance and data extraction is sometimes time consuming.

IDS GeoRadar (part of Hexagon), a provider of radar technology in the mining industry, has developed a hyper definition radar – underground, HYDRA-U radar, as a complementary instrument. It is a portable and contactless remote monitoring system, capable of providing continuous accurate measurement of small deformations over extended areas for the early detection of ground collapse in underground mines. In this paper, the relevant technology is presented together with a case study.

DEFORMATION MONITORING UNDERGROUND

Many fatalities in underground mine are hangingwall related, and workers are often exposed to falling rocks. In all the steps of the mining process, the miners have to be constantly aware of their position in relation to the hangingwall supports, the last line of defence. Strata control consists of examination, identification of hazards, inspection, support, monitoring and proper safety procedures while mining. The examination consists mainly in the identification of the geological structures of the area, such as angle joints, faults, dykes, domes, shear zone and potholes. The intersection between these structures can form blocky structures and wedges that require a lot of barring and support. Furthermore, domes and low angle joints, which are upside-down saucer shaped structures in the hangingwall, are difficult to identify and often remain hidden until a fall of ground occurs. The identification of hazards is fundamentally choosing the best support, and that will depend on the rock types, and the geotechnical characteristic of the area if the sector will be used by mining crews and others.

The inspection, usually carried out manually, consists of barring, sounding and washing to reveal and identify unstable rocks. The initial entry into a blasting heading is one of the most dangerous situations because of loose rocks. For this reason, ventilation and washdown with close visual inspection to remove fine dust and particles facilitating the detection of loose material and using both visual and sounding techniques, is important. In conventional monitoring, barring down is the first line of protection against rock fall. Deformation measurement, in most cases, still relies on contact sensors and the collection of data may require the physical collection of sensor data on-site. The installation of these devices can cause operational downtime in the sector and exposes other personnel to the dangers of the underground environment for long periods, even days.

HYDRA-U is a radar specifically designed and developed for rock mechanic engineers in underground mining, Cecchetti et al (2017), and it is a remote monitoring system capable of providing accurate measurements of small displacements of spatial areas for the early detection of ground collapse. The remote connection enables checking of the monitoring areas, so that operators can access the working zone knowing which sectors are the most unstable. The system can be installed in an area declared as safe, without the need for reflectors or markers having to be installed in the monitored area; the presence of additional personnel is minimized as the installation takes only a few minutes.

Continuous monitoring can significantly improve the safety record of operational practices and the evaluation of the stability of the rock mass. By regularly providing information on the condition of the underground areas, monitoring can help identify local failures, detect problems and their location, and enable maintenance and repair operations to be carried out in time. Maintenance cost is optimized, and economic losses are decreased.

System description

The main technical features of HYDRA-U are:

- Scan speed: a new acquisition is performed every 30 seconds.
- Spatial coverage: horizontal field of view of 120° and vertical of 30°. Radar head can be tilted ±30° to extend the maximum reach of the system in the vertical alignment.
- Spatial resolution: monitored area is divided in resolution cells of 0.20 m × 0.08 m for distances up to 10 m from the radar and 0.20 m × 0.40 m at 50 m.

- Accuracy: line-of-sight displacement with an accuracy better than 0.1 mm, providing an updated displacement heat map immediately after every acquisition.

- Survey: the 3D surface model of the monitored area is created by means of an integrated laser sensor.

Figure 1 shows that HYDRA-U consists of an acquisition and a supply and control unit. The data can be visualized on-site with a tablet or through a remote connection from the office.

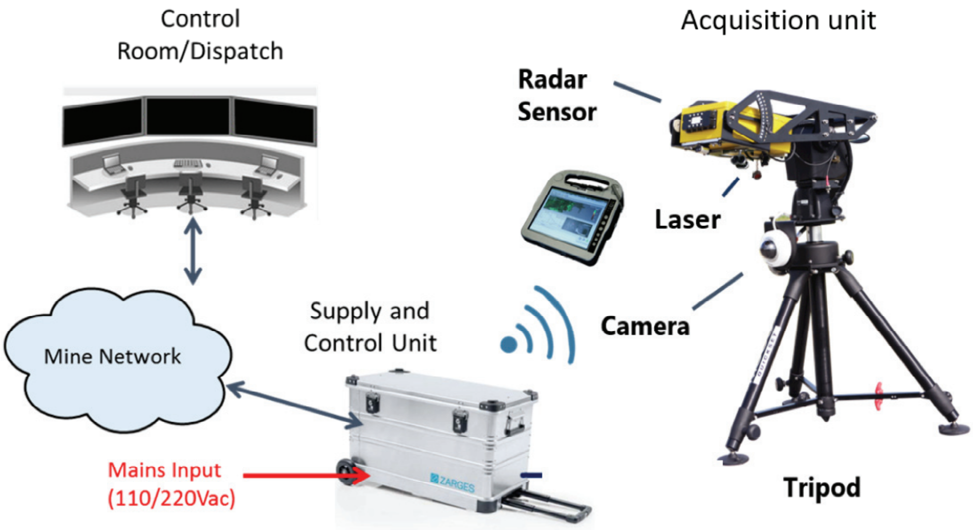

Figure 1. Acquisition and supply and control unit

The acquisition unit consists of three sensors: a radar head, infrared camera and laser. With a pan/tilt module, the radar can perform the selected acquisition report (SAR) function, while the infrared camera continuously provides visual feedback of the monitored area, even in complete darkness. Finally, the laser unit is used to survey the 3D model of the area, on which the heat map produced by the radar is overlaid. The supply and control unit performs the real-time data processing and enables the network interfaces to remotely control the system.

Both acquisition software (Controller) and processing software (Guardian), run on an on-board integrated industrial computer. The processed data coming from the three sensors can be visualized together on a rugged tablet by wireless connection, or remotely on a desktop PC. Guardian is a monitoring platform which enables the user to quickly interpret and react to the information delivered by HYDRA-U radar monitoring. After each acquisition (of 30 seconds in duration), updated information is visualised by means of an interactive heat map that can be customised to show displacement, velocity and acceleration (See Figure 2).

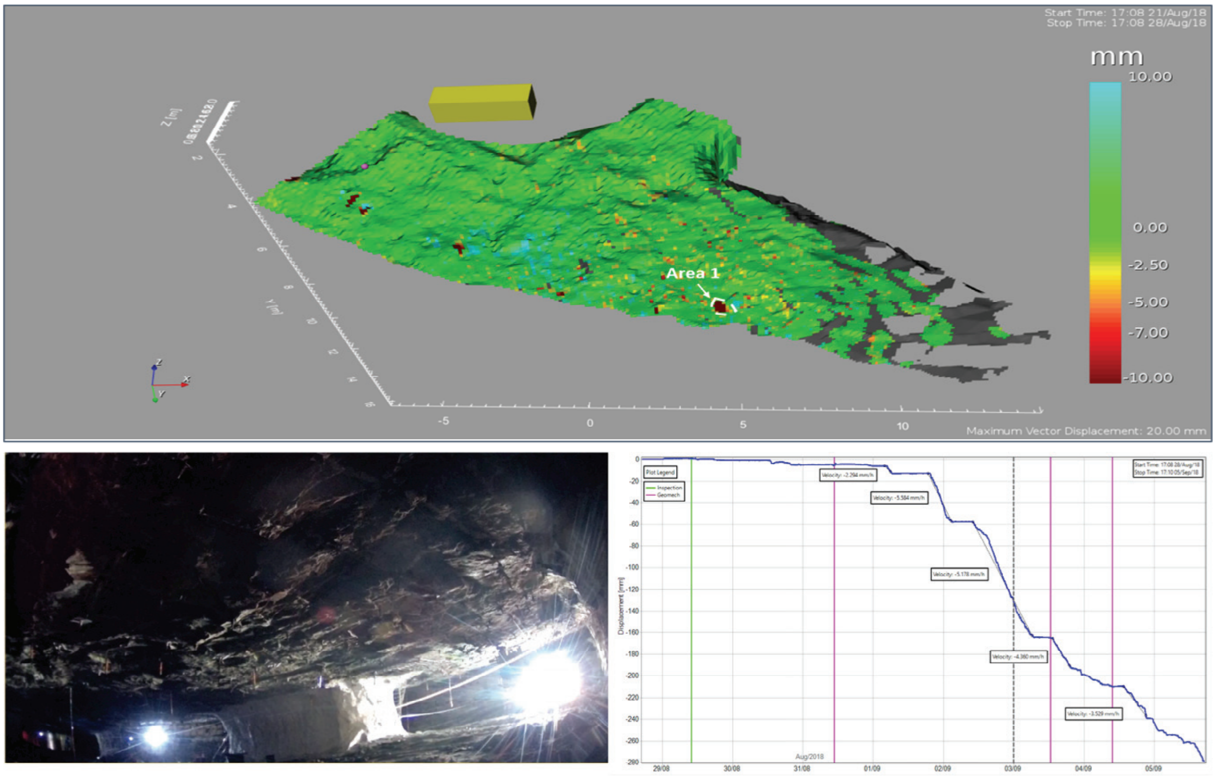

Figure 2. HYDRA-U displacement map: the radar displacement data are overlaid onto a 3D surface model produced by the integrated laser scanner

Time series graphs for specific points or areas on the map can be extracted and visualised in real time, alongside the radar maps. To assist with the interpretation and localisation of moving areas, the displacement heat map is draped onto the 3D model of the monitored surface created by the integrated laser sensor. The level of hazard of the monitored area can be managed through the definition of alarms based on user-defined velocity thresholds. Alarms can be unique for the entire scenario or area-defined to consider different geotechnical/geological area or movement direction. Each alarm activates a specific pop-up message; the alarm may also be coupled with the activation of a local audio/visual siren or transmission of a specific email message. The setting of alarms can be merged with the trigger action response plan (TARP) and create levels for geotechnical hazard and mine control.

Spatial resolution

The HYDRA-U system is designed to remotely measure displacements with sub-millimetre accuracy. Like any other radar system, it is an instrument capable of detecting the presence of objects and measuring the relative distances between the apparatus and the objects. HYDRA-U performs this task by emitting continuous radio waves with a variable frequency, linear frequency modulated continuous wave (LFMCW), and comparing the received echo frequency with the transmitted wave.

The difference between the two frequencies is proportional to the two-way flight time from the apparatus to the target, and thus to the distance between them.

Range resolution, i.e., the ability to distinguish close targets along the line-of-sight of the radar, depends on the transmitted bandwidth, and for HYDRA-U this is 0.20 m.

Cross-range resolution, i.e., the ability to distinguish close targets perpendicular to the line-of-sight of the radar, is obtained by means of the SAR technique. However, differently from other IDS GeoRadar systems for slope monitoring in open pit mines such as IBIS (See Escobar et al (2013); Farina et al (2011); Mononen et al (2016) and Ramsden et al (2015)), HYDRA-U uses the motion of the radar antenna over a circular trajectory to provide finer angular resolution than conventional beam-scanning radars ,Coli et al (2018).

The circular trajectory used for obtaining the synthetic aperture (often denoted as ArcSAR), permits a more compact design of the radar and a wider angular coverage than the traditional linear SAR. These features prove particularly crucial in underground mine environments, where transportability and compactness of the system is a must, and where the reduced available distance between the system and the wall to be monitored requires a wide field of view.

The combination of range and cross-range resolution allows the creation of a bi-dimensional image, where each pixel is a measurement point providing real-time displacement information. The overlap of the range–cross-range image on the digital elevation model registered by the integrated laser sensor produce a 3D representation of the radar map.

Deformation measurement
HYDRA-U measures the amplitude and the phase of the signals reflected by the monitored scenario; the amplitude provides information about the strength of the reflected signal, whereas the phase can be related to the relative movement of the target towards or away from the radar. The displacement magnitude is obtained with the interferometric technique, which relates the phase measurement difference that occurs between a first and a second acquisition (See Figure 3) to the line-of-sight displacement of the monitored surface according to the following equation:

$$d = -\frac{\lambda}{4\pi}(\varphi_2 - \varphi_1) \quad (1)$$

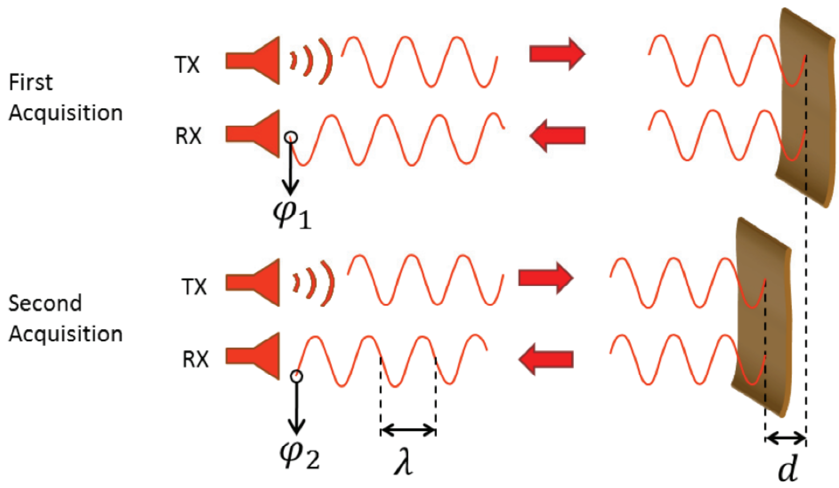

Figure 3. Displacement measurement using radar interferometry

The accuracy on the displacement measure d depends on the phase measurement accuracy φ and on the value of the transmitted signal wavelength λ. HYDRA-U is capable of providing displacement measurement with an accuracy better than 0.1 mm, by combining a very high phase measurement accuracy (< 0.1 radians) to a short wavelength (4 mm). After any acquisition, HYDRA-U gives a displacement measure of any resolution cell within the field of view of the system.

Operating results: an underground case study
HYDRA-U is shown, monitoring a specific area inside the mine with the goal of measuring displacement of a specific area. Figure 4 shows the system installed on a tripod and how it is possible to visualize the radar data on the tablet using a wifi connection.

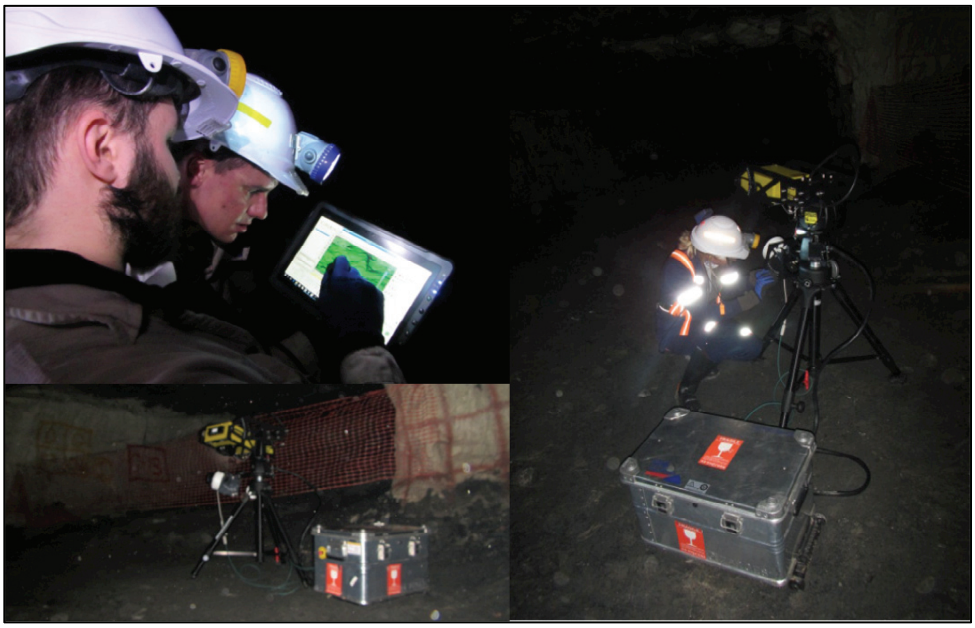

Figure 4. Installation of Hydra-U

The mining cut along the entire area is almost constant and it varies between 2,5 m and 3 m . In the sector, other instrumentation such as mechanical closure meters, extensometers, strain gauges, geophones, borehole cameras and rock spy instruments are installed. The collection of measured data is performed manually on a daily basis. Since the measurements are indirect, post-processing of the data is required. The monitored area is prone to strain burst associated with pothole intrusions. The area is also affected by the continuous passage of personnel and machines due to operations in that area. This case study shows the radar data and displacement of small portions of falling rocks. It does not show analysis from other installed instruments. Displacement maps obtained by the radar image of the area captured by the infrared camera and analysis on Guardian software are shown. In the time interval between 20 June and 4 July 2018, two areas have shown a significant deformation rate (See Figure 5).

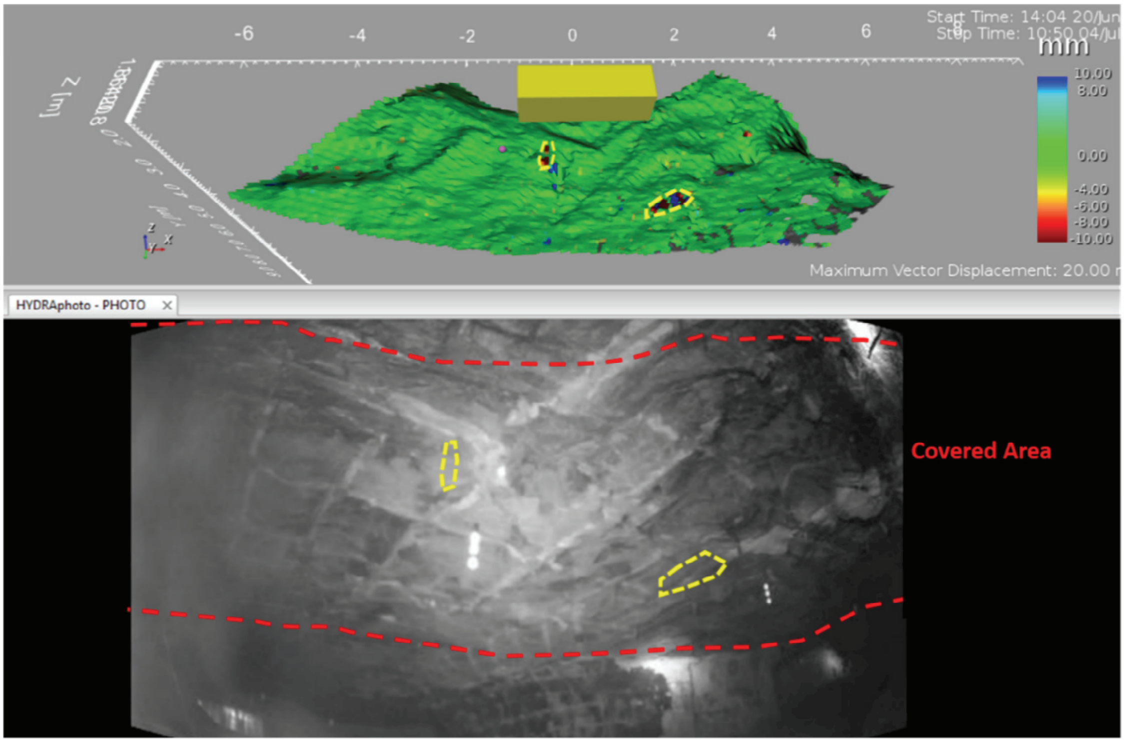

Figure 5. Correlation between moving areas on the displacement map and moving areas on the photograph

Displacement is expressed in millimeters. By default, the approaching negative is set: this means that a negative displacement (warmer colors) corresponds to a movement towards the radar. The green color means that there is no noticeable movement in both directions.

To have a better understanding of the nature of the displacements, several points were considered inside the two sectors: in area 1, two points were considered: Point 3 and Point 5. In area 2, four points were considered: Points 1,2,7 and 8. In area 1, (Figure 6), the displacement time series of Point 3 and Point 5 are represented. The location of these points is visible on both on the displacement map and the infrared photo taken by the HYDRA-U camera.

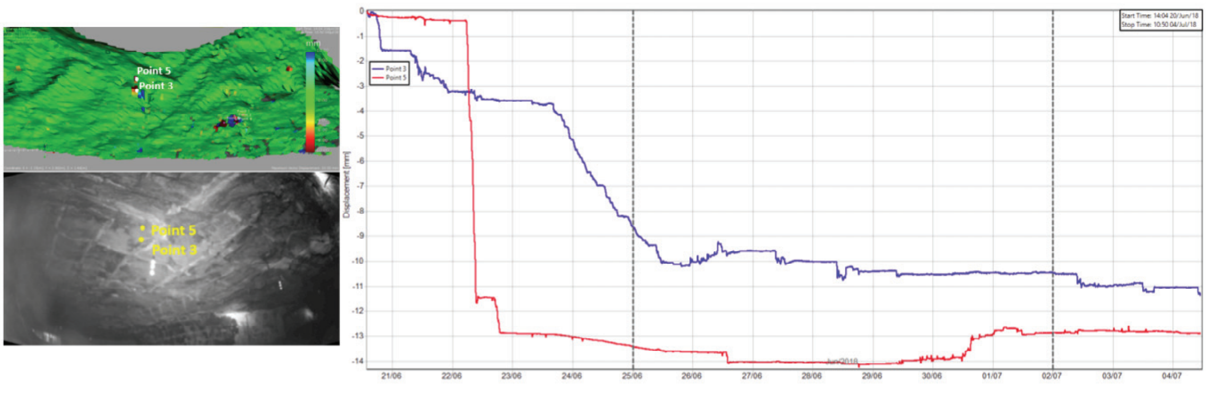

Figure 6. Displacement time series of Points 3 and **5**

Points 3 and 5 show between 11 and 13 millimetres of displacement within the analysed time interval (14 days). Point 5 shows a high rate of displacement, more than 11 mm of displacement in 4 hours (between 5 am and 9 am on June 22). The average velocity within this trend is 2.83 mm/h (See Figure 7).

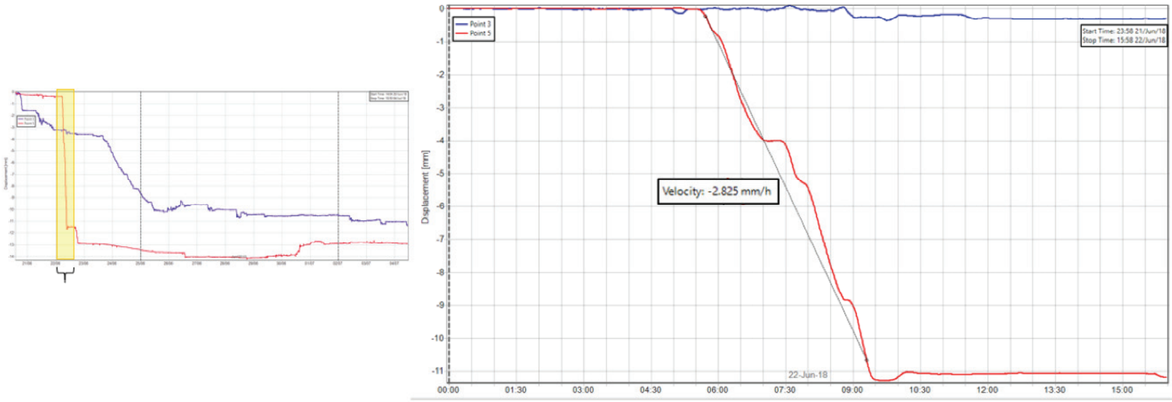

Figure 7. Zoom on the acceleration trend of the displacement time series relevant to Point 5

Point 3 shows a linear trend of displacement, 6 mm of displacement within a time window of 2 days and 7 hours (between June 23 at 4.30 pm and June 25 at 11.30 pm). The average velocity within this trend is 0.14 mm/h (See Figure 8).

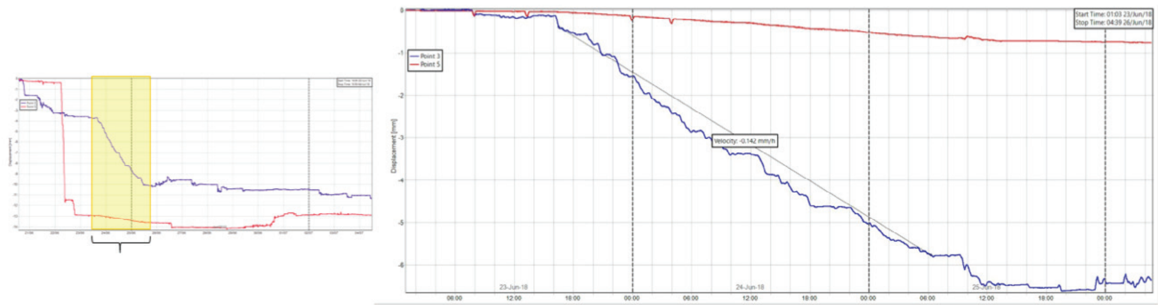

Figure 8. Zoom on the acceleration trend of the displacement time series relevant to Point 3

In the second area, four points were considered: Points 1, 4, 7 and 8.
In Figure 9 their displacement time series is shown. The locations of these points are visible both on the displacement map and on the infrared photo.

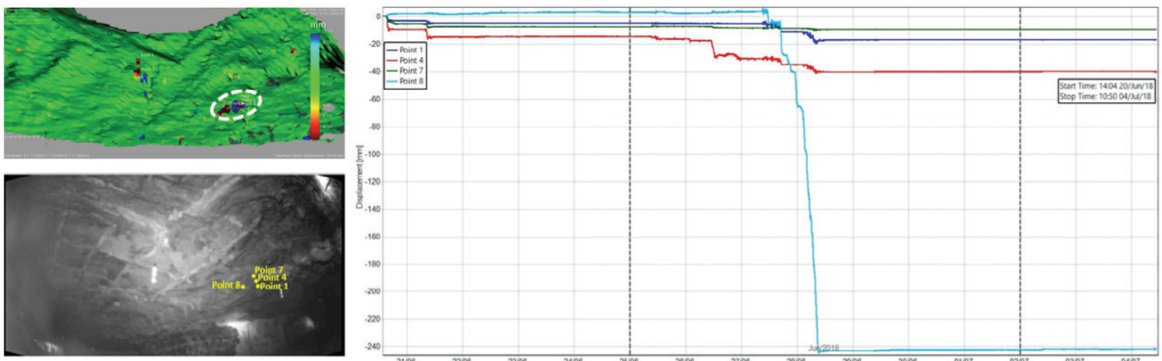

Figure 9. Displacement time series of Points 1,4,7 and 8

Points 1 and 7 are stable compared to Points 4 and 8 which show significant movement over the considered time interval. Point 4 shows a steep linear trend, with a displacement of almost 12 mm within a time window of 2 hours (from June 26 at 11 am to 1 pm). The average velocity within this trend is about 7.10 mm/h (See Figure 10).

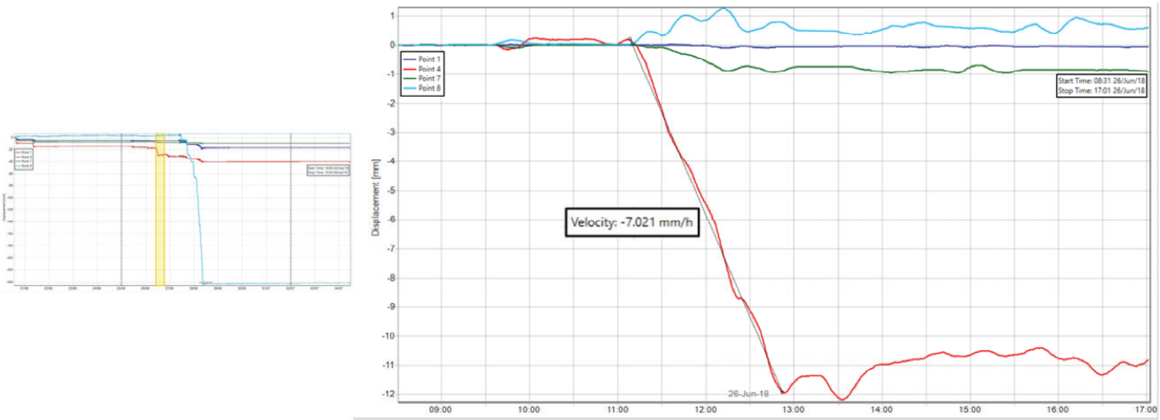

Figure 10. Zoom on the acceleration trend of the displacement time series relevant to Point 4

Point 8 shows a stepped displacement trend starting from June 27th at 11.30 am to June 28th at 10 am, with a displacement of almost 250 mm within a time window of 23 hours. The average velocity within the acceleration phases is between 27 mm/h and 32 mm/h.

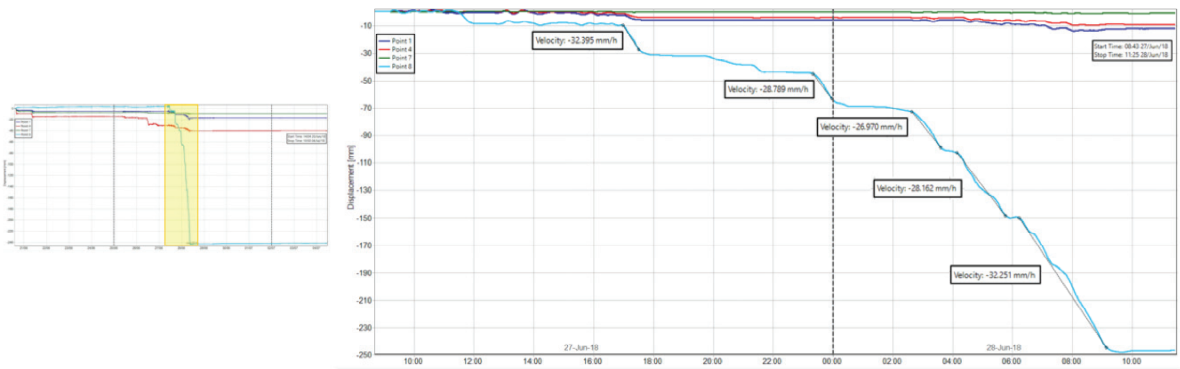

Figure 11. Zoom on the acceleration trend of the displacement time series relevant to Point 8

SUMMARY

Considering the time interval between June 20 and July 4, two areas show a significant displacement rate. In the first area, Point 3 shows a linear trend of displacement, 6 mm of displacement within a time window of 55 hours with an average velocity of 0.14 mm/h ,while Point 5 shows a high rate of displacement - more than 11 mm of displacement in 4 hours with an average velocity of 2.83 mm/h.

In the second area Point 1 and Point 7 are almost stable, while Point 4 and Point 8 show a significant displacement: Point 4 shows a steep linear trend, with a displacement of almost 12 mm within a time window of 2 hours with an average velocity of 7.10 mm/h. Point 8 shows a stepped displacement trend with a displacement of almost 250 mm, within a time window of 23 hours.

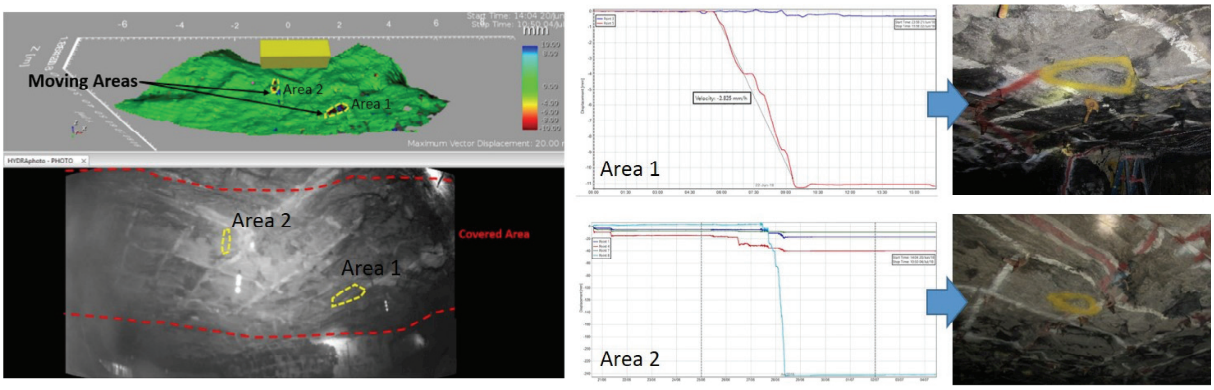

Figure 12. Case studies

A report containing the above mentioned data was sent to the chief rock engineer who was able to check the moving areas together with the mining crew, and safely barring down the sectors that had been identified and marked by the underground crew.

CONCLUSIONS

Many fatalities in underground mines are hangingwall-related, and workers and machinery are constantly exposed to falling rocks. HYDRA-U is a complementary instrument capable of providing answers where there is an increased need for accuracy and reliability in monitoring underground tunnels and stopes. As shown in the case study, the use of HYDRA-U allowed the mining crew and chief rock engineer to identify unstable areas before entering the sector. Continuous monitoring can significantly improve the safety of operational practices and the evaluation of the stability of the rock mass. By regularly providing the information on the conditions in the underground areas, monitoring can help prevent local failures, detect problems and their locations, maintenance and repairs operations can be carried out in time. The result is that maintenance cost is optimized, and financial losses are decreased.

ACKNOWLEDGEMENTS

The authors thank the mine, the chief rock engineer, the senior rock engineer and the mine technical manager who worked shoulder to shoulder with us, and for permission to use the data and images included in this paper.

REFERENCES

Cecchetti, M., Rossi, M., Coppi, F., Bicci, A., Coli, A., Boldrini, N. and Preston, C. (2017), 'A novel radar-based system for underground mine wall stability monitoring', in M. Hudyma and Y. Potvin (eds), *Proceedings of the First International Conference on Underground Mining Technology, Australian Centre for Geomechanics*, Perth, pp. 431-443.

Bernardini, G., Ricci, P. and Coppi, F. (2007). 'A ground-based microwave interferometer with imaging capabilities for remote measurements of displacements', *Proceedings of the 7th Geomatic Week*.

Brink, V.F. ,Fourie, F. ,Mine, K. and Zaniewski, T. (200)8. *Continuous Monitoring for Safety, Health and Optimisation in South African Deep Level Mining*, Southern African Institute of Mining and Metallurgy, pp. 1–15.

Brady, B. and Brown, H. (2005). *Rock Mechanics for Underground Mining*, 3rd edn, Springer Science+Business Media, Berlin.

Coli, N., Leoni, L., Coppi, F. and Preston, C. (2018). 'Evolution of Synthetic Aperture Radar technology for safety-critical monitoring in open-pit mines, *Proceedings of the 2018 International Symposium on Slope*

Stability in Open Pit Mining, Australian Centre for Geomechanics, Seville, Spain, April 10-13, 2018.

Escobar, A., Farina, P., Leoni, L., Iasio, C. and Coli, N. (2013). 'Innovative use of slope monitoring radar as a support to geotechnical modelling of slopes in open pit mines', in PM Dight (ed.), *Proceedings of the 2013 International Symposium on Slope Stability in Open Pit Mining and Civil Engineering*, Australian Centre for Geomechanics, Perth, pp. 793–802.

Farina, P., Leoni, L., Babboni, F., Coppi, F., Mayer, L. and Ricci, P. (2011). 'IBIS-M: An innovative radar for monitoring slopes in open-pit mines', *Proceedings of the 2011 International Symposium on Rock Slope Stability in Open Pit Mining and Civil Engineering*, Canadian Rock Mechanics Association, pp. 18–21.

Kumar, A., Kumar, D., Gupta, P. and Shankar, G. (2011). 'Optimizing fibre optics for coal mine automation', *International Journal of Control and Automation*, vol. 4, no. 3, pp. 19–30.

Kukutsch, R., Kajzar, V., Konicek, P., Waclawik, P. and Ptacek, J. (2015). 'Possibility of convergence measurement of gates in coal mining using terrestrial 3D laser scanner', *Journal of Sustainable Mining*, vol. 14, no. 1, pp. 30–37.

Maleki, H. and McVey, J. (1988). *Detection of Roof Instability by Monitoring the Rate of Movement*, *Bureau of Mines Report of Investigations RI 9170*, U.S. Government Printing Office, Washington

Moffat, D.C., Beltran, R. F. and Herrera, R. (2015). 'Applications of BOTDR fiber optics to the monitoring of underground structures', *Geomechanics and Engineering*, vol. 9, no. 3, pp. 397–414.

Mononen, S., Suikkanen, M., Coli, N., Funaioli, G. and Meloni, F. (2016). 'Critical Real Time Radar Monitoring of Sub-bench Failures at Yara Suomi Oy Siilinjärvi Open Pit Mine (Finland)', in Ulusay, R., Aydan, Ö., Gerçek, H., .,Hindistan, A.M., and Tuncay, E. (eds), *Proceedings of EUROCK 2016: Rock Mechanics and Rock Engineering: From the Past to the Future,* Taylor & Francis Group, London.

Mines Occupational Safety and Health Advisory Board (1997), *Geotechnical Considerations in Underground Mines*, Document No.: ZME723QT, Department of Industry and Resources, Perth.

Mine Safety and Health Administration (2015), *Lost-time Injuries by Accident Class for Surface and Underground Mining Locations,* Mine Safety and Health Administration, Atlanta, viewed 25 July 2017, https://www.cdc.gov/niosh/mining/statistics/allmining.html.

Ramsden, F., Coli, N., Benedetti, A.I., Falomi, A., Leoni, A.L. and Michelini, A. (2015). 'Effective use of slope monitoring radar to predict a slope failure at Jwaneng Mine, Botswana', *Proceedings of the 2015 International Symposium on Slope Stability in Open Pit Mining and Civil Engineering*, The Southern African Institute of Mining and Metallurgy, Johannesburg.

Slaker, B. (2015). *Monitoring Underground Mine Displacement Using Photogrammetry and Laser Scanning*, PhD dissertation, Virginia Polytechnic Institute and State University, Blacksburg.

Szwedzicki, T. (2008). 'Precursors to rock mass failure in underground mines', *Archives of Mining Sciences*, vol. no. 3, pp. 449–465.

Noemi Boldrini

Business Developer
IDS GeoRadar

Noemi Boldrini is a geotechnical geologist, who built her career in a variety of roles in the geology sector, industries and countries. She is currently working as a business developer with the aim of developing worldwide new business opportunities of new products in underground and in open pit mines, working directly with clients to meet their needs.

Identifying relevant ground movement monitoring requirements

D.N. Nyungu and P. Pastorino

New Concept Mining, South Africa

Some of the factors that influence rock mass deformation induced by stress redistribution, include mining method, installed ground support and properties of the rock mass. Mining operations use numerical simulation at the mine design stage as one of the tools to evaluate these influences. There is a need to quantify movement incurred by the rock mass during design implementation to evaluate the performance of installed ground support. This in light of potential unwanted damage to excavations and to give relevant early warning in response to excessive deformation. This paper will present the benefits of carefully planned in situ ground movement monitoring in mine design, validating numerical modelling and evaluating ground support performance. Ground movement monitoring in the first instance can serve as an early warning signal of potentially unsafe ground conditions.

INTRODUCTION

The advance of a mining face redistributes stress by altering the condition of the surrounding rock mass. Mining-induced rock mass deformation is influenced by many factors, such as the pre-mining stress profile, the mine layout, the excavation profile, the rock mass elastic modulus, the properties of geological discontinuities and the characteristic performance of the installed support.

Ground monitoring devices are essential in a mining life cycle to quantify local rock mass behaviour and assess the impact of implementing new designs and procedures, Jager and Ryder (1999). Recently, ground monitoring devices have also been used to back-analyse certain rock mass behaviour, Song et al (2016). It is imperative to be able to identify the relevant ground movement monitoring parameters, to measure the expected impact on installed support resulting from mining-induced rock mass deformation. Early warning triggers prior to damaging deformation are required to manage the risk of unstable excavations. In this study the different aspects of ground movement monitoring are highlighted.

Deformation due to mining-induced stress

Stress is transferred through a solid medium and its trajectory is influenced by the shape of openings where the solid medium has been removed. The pre-mining stress can be categorized as virgin and induced stress (See Figure 1).

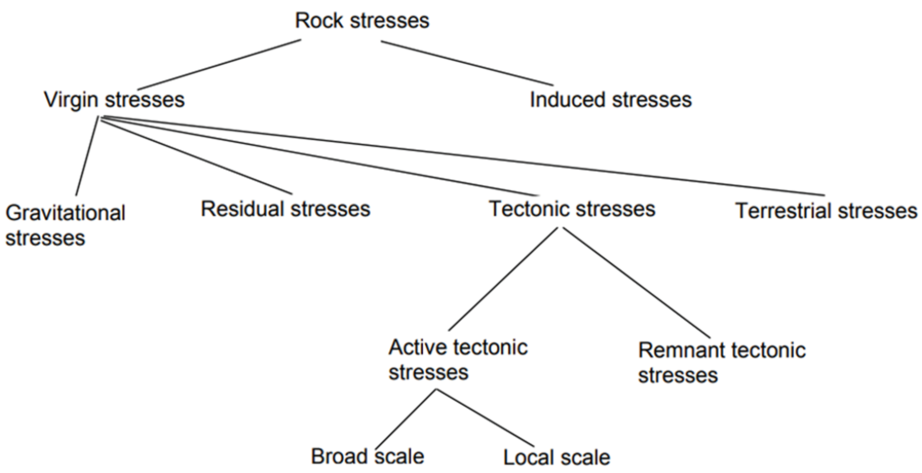

Figure 1. Basic stress terminology, after Amadei and Stephansson (1997)

To introduce the concept of rock mass deformation as a response to induced stress, see the following basic illustrations of stress redistribution in Figure 2.

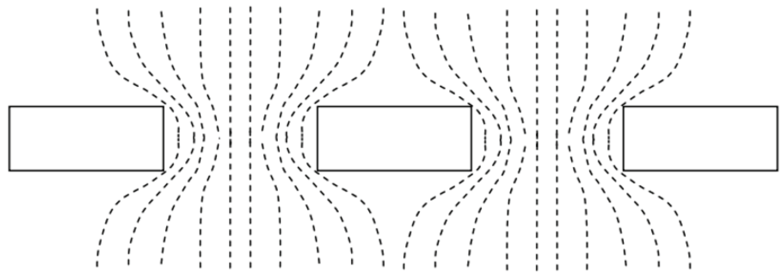

Figure 2. Stress contours around parallel rectangular tunnels, after Larsson (2004)

Principal stresses are overall either vertical or horizontal, but they do not always conform to these geometric orientations. Principal stress orientations at different stages of mining past a footwall drift are schematically depicted in Figure 3.

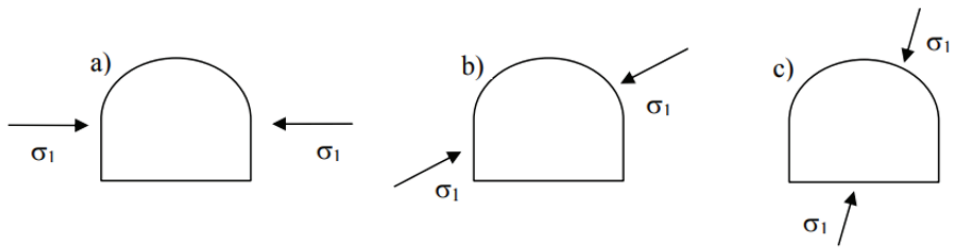

Figure 3 - Rotation of stress field during the life of a footwall drift (a) at development stage (b) production has reached the same level as the drift, and (c) extraction passed the drift by 100 m or more. After Larsson (2004)

The induced stress profile influences the excavation rock boundaries by way of deforming the rock mass, governed by the rock mass elastic modulus until a new state of equilibrium has been reached (See Figure 4).

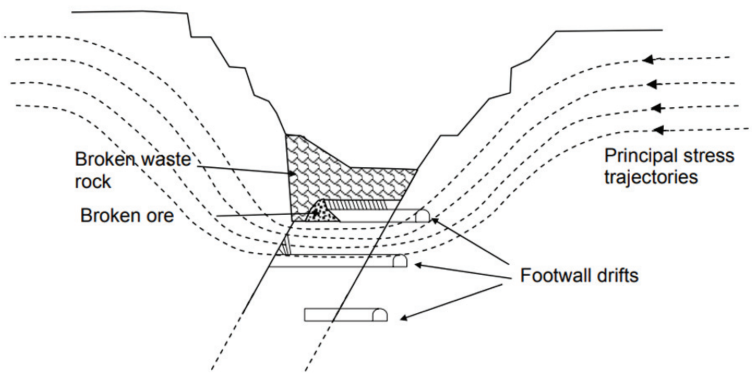

Figure 4. Schematic depicting stress redistribution under a caved zone, after Larsson (2004)

Mine operations have to establish site-specific deformation characteristics through instrumented monitoring of the relevant rock mass response to mining-induced stress. Early warning triggers can therefore be incorporated as visual methods prior to predetermined damaging deformation occurring.

Squeezing ground conditions
Squeezing ground conditions are a result of the impact of induced stress on weak rock mass strength with perceptible reduction in excavation dimensions. Descriptions of squeezing ground based on perceptible tunnel strain are given by Aydan et al (1993), with distinction between failure modes detailed as; complete shear, buckling, shearing and sliding failure (See Figure 5).

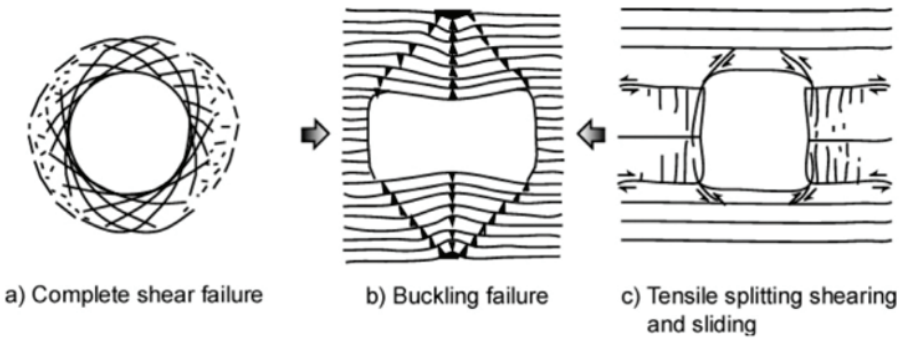

Figure 5. Classification of failure observed in tunnels in squeezing ground conditions, after Aydan et al (1993)

The phenomena summarized in Figure 5, contributes to measurable deformation in an excavation. Certain levels of deformation become critical to excavation stability and function. Table I depicts a summary of the classification for squeezing potential based on strain and strength index measured in a tunnel, both are good indicators of imminent failure in a tunnel, Aydan et al (1993); Hoek (2001) and Singh et al (2007).

Table I. Classification for squeezing potential in tunnels

Class #	Hoek (2001)		Aydan *et al.* (1993)		Singh *et al.* (2007)	
	Squeezing level	Tunnel strain	Squeezing level	Tunnel strain	Squeezing level	*SI*
1	Few support problems	$\varepsilon_t < 1\%$	No squeezing	$\varepsilon_\theta^a/\varepsilon_\theta^e \leq 1$	No squeezing	$SI < 1.0$
2	Minor squeezing problems	$1\% < \varepsilon_t < 2.5\%$	Light	$1 \leq \varepsilon_\theta^a/\varepsilon_\theta^e \leq 2.0$	Light	$1.0 < SI \leq 2.0$
3	Severe squeezing problem	$2.5\% < \varepsilon_t < 5\%$	Fair squeezing	$2.0 \leq \varepsilon_\theta^a/\varepsilon_\theta^e \leq 3.0$	Fair squeezing	$2.0 < SI \leq 3.0$
4	Very severe squeezing problem	$5\% < \varepsilon_t < 10\%$	Heavy squeezing	$3.0 \leq \varepsilon_\theta^a/\varepsilon_\theta^e \leq 5.0$	Heavy squeezing	$31.0 < SI \leq 5.0$
5	Extreme squeezing problem	$\varepsilon_t > 10\%$	Very heavy squeezing	$\varepsilon_\theta^a/\varepsilon_\theta^e > 5.0$	Very heavy squeezing	$5.0 < SI$

In squeezing excavation design, strain criteria have gained preference over strength criteria considering the relative ease of measuring of rock mass deformation, Hoek (2001) and Potvin and Hadjigeorgiou (2008). Hoek (2001) demonstrated that recorded strain could be used as a tool to predict squeezing potential. As an example, Potvin and Hadjigeorgiou (2008) quote a 2% strain, based on 10 cm deformation in a 5 m x 5 m tunnel, as typical squeezing ground conditions in excavations with similar dimensions. This suggestion was based on case studies by Potvin and Slade (2007); Mercier-Langevin and Turcotte (2007) and Sandy et al (2007). A preset critical rock mass strain level, based on measured deformation history, should form a sound basis for risk management in squeezing ground. Early warning devices can be put in place to warn of such critical rock mass strain levels approaching.

Deep hard rock mining conditions
Hard rock in engineering projects under deep, high ground stress conditions, shows obvious creep properties and time effects. See Liu (1994); Yao (2005) and Nyungu and Stacey (2014). A high rate of deformation is observed with deep level mining in hard rock as fractures dilate and propagate with resultant changes observed in the excavation shape and size. Depending on the rate of deformation or release of energy around an excavation, yielding or dynamic conditions may prevail (See Figure 6).

(a) Yielding ground conditions

(b) Catastrophic failure of back and rock bolts

Figure 6. Different rock mass response to deformation at high stress, after Charrette and Plouffe (2008)

These conditions are candidate for continuous monitoring and perhaps intermittent or continuous feedback, with early warning triggers.

Yielding ground conditions
Yielding conditions can result from creep in solid rock and many researchers have studied the creep properties of rock. Under yielding conditions (See Figure 6 (a)), the support unit gradually strains while maintaining load within its strength capacity. Griggs (1939) showed that creep occurs in sandstone, shale, and silty sandstone rock under the load of 12.5 % – 80 % of the failure load. Subsequently, more research was published on rock creep tests, including: the uniaxial compressive creep test, the triaxial

compressive creep test, the discontinuity rock shearing test, and field tests, Wawersik (1974); Amadei and Curran (1980); Okubo et al (1991); Jin et al (1995), Brazilian indirect tensile (BIT) strength tests and Nyungu and Stacey (2014). Nyungu and Stacey investigated the long-term strength of several Bushveld Complex rock types which further illustrated the need to measure associated deformation in the rock mass.

Dynamic ground conditions
Under dynamic loading conditions (See Figure 6 (b)), a sudden high impact load is instantaneously imparted onto the support system, with residual load from loosened rocks expected after the impact has been dissipated by the energy absorption capacity of the support. Two scenarios of deformation monitoring arise - continuous and instantaneous. The latter being affected by the accuracy of the placement of monitoring devices, and the timing and potential direct damage to measuring devices due to a high energy impact. This raises the question whether it is ever critical to measure the damage imparting energy itself or rather the resultant measurable impact on the observed rock mass and support. Quantifying the measurable deformation in a rock mass and installed support aids informed excavation and support design. Early warning for critical damaging conditions becomes essential to avoid high rehabilitation costs. It is essential to be able to measure the strain experienced by the rock mass compared to the original excavation dimensions and that sustained by the support elements.

Shallow low-stress mining conditions
Deformation in hard rock low-stress mining conditions may not be as easily observable compared to weaker squeezing rock mass conditions or in high-stress hard rock conditions. However, it does not absolve the importance of measuring the deformation on intact rock, including movement on discontinuities and resultant large-scale movement of blocks as a result of mobilized structures with low or no clamping forces. Low-stress mining conditions require intermittent monitoring and intermittent feedback with early warning triggers, as the deformation rates are much slower than both earlier cases discussed.

Deformation monitoring and early warning at low trigger levels should therefore be a part of the low-stress mining risk management. A standard method of visualizing the rock mass loading conditions and expected critical deformation characteristics, is through simulation of different mining environments depicting investigated conditions. Lately simulation has been replaced by numerical analysis following advancements in data processing speed.

NUMERICAL SIMULATION OF DEFORMATION

Numerical simulation has a shorter feedback turnaround on rock mass deformation information compared to in situ measurements, the later spanning short-term to long-term periods ranging minutes to years. Theoretically, deformation and its impact on installed support can be modelled with relatively good correlation to perceivable mining conditions. Many numerical software tools such as UDEC Munson (1997); ANSYS Liu and Sun (1998) and FLAC3D Gao et al (2000), can be applied to rheological analysis in geotechnical engineering. A rock failure process analysis (RFPA) system for the simulation of failure processes and the time effect of surrounding rock in tunnels was developed by Ma et al (2013). However, because of the uncertainty and complexity of geological bodies, the adoption of the relevant model and rock mass parameters is the key factor affecting the accuracy of numerical simulations in underground engineering.

There is growing interest in back-analysis using displacement data from monitoring of the surrounding rock to identify rock mechanics parameters, Boydy and Bouvand (2002), and Moyo (2018). Rock creep parameter back-analysis methods were studied by Sakurai (2009); Mostafa et al (2013) and Montassar and Buhan (2013). Sakurai (2009), back-analysed rock mass creep parameters using field monitoring data. For numerical simulation to be realistic and applicable to mining it has to be based on measured calibration parameters and post-validated against observed measured deformation. The pre-determined critical deformation levels from numerical analysis can therefore be incorporated into early warning devices averting damaging deformation and warning of required support rehabilitation.

EXCAVATION AND SUPPORT DEFORMATION

The extent of the plastic damage zone around an excavation depends on various factors. Some factors are easily predictable through laboratory and simulation runs thus controlled. Others are a result of inherent rock mass conditions thus often uncontrolled. It is thus imperative to be able to identify the relevant deformation parameters to set up the correct ground movement measuring and feedback protocol for each mining operation.

Deformation of mine support

In mine design, the mine engineer has to be able to quantify the interaction between installed support and the rock mass, one influencing the other's behaviour. Deformation of support elements under dynamic or static loading can be measured with a relatively high degree of accuracy using dynamic impact Knox et al (2018) or static tensile tests. The significance of being able to predict the deformation needed for a given dynamic event based on the energy and the expected area or mass involved is that a preventive design can be performed and the desirable tendon properties can be chosen to match expected requirements, Charrette and Plouffe (2008). However, these tests are often based on an individual tendon loading and not a system loading that includes the fabric of the surface support utilized. In situ deformation measurements indicate the system deformation characteristics.

Monitoring loads on rock bolts and movements within a tunnel can provide an indication of the stability of the tunnel, Cabalar et al (2012) and Argyroudis et al (2013). Determination of the influence of the redistribution of the stress locked up in a rock mass on support units is possible through monitoring, something that numerical simulation has limitations. In-situ deformation measurements therefore become critical in back analysis of support systems. Overall one has to use the deformation information to decide on critical support deformation beyond which rehabilitation or replacement is required.

Impact of blasting on deformation

The impact of blasting on rock mass deformation has been documented by several researchers, notably Jones et al (2019). The location of the blasts relative to the monitoring device (or a particular location) is an important variable influencing some of the relationships governing deformation, Jones et al (2019). According to a study by Jones et al (2019), the redistribution of mine stresses has a greater impact on deformation than does blasting damage proximity. Notwithstanding the potential for a hit or miss, Millis et al (2009), with monitoring device location, most instruments are not required to be located at the source of the trigger being measured, only to measure the resultant deformation.

DEFORMATION MEASURING

Ground monitoring devices are used in recording initial conditions in an excavation prior to mining, including fracture conditions, load-in support, field stress, rock field strength, and joint properties. A wide range of parameters can be measured as long as a preset monitoring signal is determined and a means to record the signal and process the data is available. Often these systems require a power source or an analogue sensing system that can be directly visually read off the instrument or alternatively sent out to a processing system located at a remote site.

Monitoring device criteria

A great deal of study has been completed in the fields of monitoring instruments underground by Maghsoudi and Kalantari (2014); and process monitoring underground by Johansson (2010). It must be noted here that different instruments of varying accuracy, precision and communication modes are selected depending on the monitoring or measuring objectives sought. Monitoring falls into short-term and long-term, dependent on the operation's requirements. Monitoring devices can be any of the following types: optical, mechanical, hydraulic, pneumatic and electrical. Robotic monitoring devices have been developed, but these are still largely reliant on the availability of a clear line of sight.

Monitoring device location, accuracy or precision, continuous or intermittent measuring and feedback, expected range and rate of change in parameters being monitored, skills levels available to install devices, skills to capture readouts, application of complimentary equipment and budget, influence the type of monitoring device chosen. The frequency of readings depends on the rate of change of the measured parameter rather than the duration of the monitoring programme. The choice of monitoring device can therefore be simplified or complicated depending on the monitoring objectives.

CASE STUDIES

Ground monitoring devices are generally of immense value during geotechnical construction, Sikora and Ossowski (2013). A case study follows quoted by Jones et al (2019) based on Sundström's work. Between May 2007 and April 2010, deformation data was acquired from a suite of 20 stress measurement to assess reinforcement tension (SMART) cable bolts installed on levels 932 and 962 of the Norra Alliansen orebody, illustrated schematically in Figure 7.

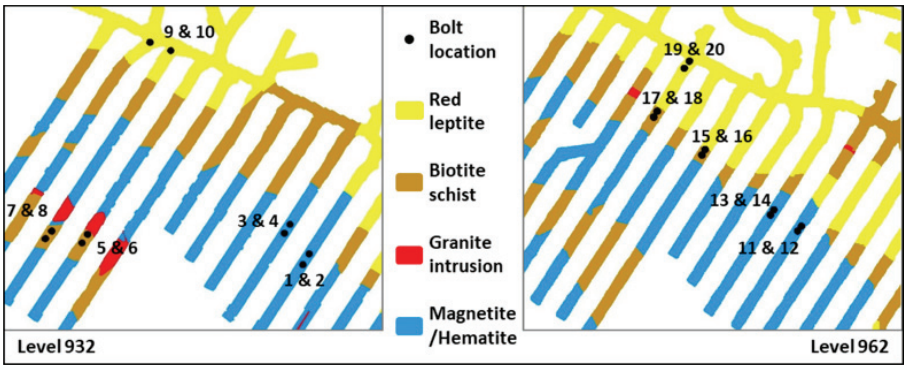

Figure 7. Geologic map showing levels 932 and 962, with installed instrument locations, after Jones et al (2019)

This case study showed how extensive monitoring device regimes are beneficial to gathering the parameter data relevant to make informed decisions. It also illustrated how critical planning of the measurable parameter is as the exercise is both labour, time and capital intensive. The exercise may hamper productivity or be a waste of time if the relevant parameter measurements are not planned. Deformation in a deep level mine in Jichuan China was measured and correlated to numerical modelling, Song et al (2016). Correlation was found between the simulated deformation and the measured deformation based on back-analysis of input parameters using the Nishihara model. Geotechnical or deformation measuring devices were used successfully during the extraction of the Ingula Power caverns project for model calibration and design verification, Kellaway et al (2012). Feedback from monitoring devices was recommended for use in the design of shallow spans, Swart and Handley (2004).

Real-time monitoring of ground movement and groundwater conditions associated with natural terrain landslides in Hong Kong was carried out by Millis et al (2009). The project was capital intensive and time consuming due to the vast area involved but brought valuable feedback and early warning leading to critical safety and evacuation decisions in the region, to mitigate landslide hazards. These cases show the importance of carefully planned monitoring regimes with focused feedback objectives. It is important to scope the monitoring objectives including feedback intervals and resolution.

CONCLUSIONS AND RECOMMENDATIONS

The following conclusions and recommendations are drawn from this study:

- Different stress and rock mass conditions result in varying deformation conditions.
- Continuous monitoring and intermittent or continuous feedback incorporating early warning triggers, are applicable to deep hard rock yielding conditions.
- Dynamic mining conditions are inclined to continuous monitoring with instantaneous feedback.
- Shallow low-stress mining conditions require intermittent monitoring and intermittent feedback with early warning triggers due to the associated low deformation rates.
- Monitoring devices in dynamic conditions are affected by the accuracy of placement and direct damage due to the proximity of impact.
- Effective monitoring should be able to validate design assumptions, validate numerical simulation parameters, confirm layout, validate support performance and give early warning for critical conditions.
- It is essential to establish the initial excavation or support dimensions and conditions as a base for monitoring to allow continued comparative strain analysis.
- The strain criteria are a viable risk management tool to give early indication of impeding critical deformation in excavations and installed support.
- Establishing the critical strain for both the excavation and the installed support units is key to mine design.
- Early warning deformation trigger systems have to be incorporated into the monitoring regime.
- A good excavation risk management tool is to use ground movement measurement to establish the need to replace support or rehabilitate the excavation.
- Based on the stage of the mining project and available monitoring budget, a decision has to be made for the duration of monitoring, the type of monitoring device used and feedback intervals together with technologies accompanying the process.
- Numerical simulation of deformation has been confirmed to be accurate in several case studies compared to deformation measured in situ.
- An all-round adoption of monitoring tethered to numerical simulation may be time-consuming and costly to introduce to matured mining projects, but it is unquestionably worthwhile incorporating from the inception of new projects.
- A modular monitoring regime targeted at specific conditions, objectives and application must be planned.
- Monitoring device location, device accuracy or precision, continuous or intermittent measuring and feedback, expected range of deformation, rate of change in parameter being monitored, skills levels available to install, skills to readout, complimentary equipment and available budget, influence the choice of monitoring device.

REFERENCES

Amadei, B. and Curran, J.H. (1980). Creep behavior of rock joints. *Proceedings of the 13th Canadian Rock Mechanics Symposium.* pp.146-150.

Amadei, B. and Stephansson, O. (1997). Rock Stress and its measurement. London: Chapman and Hall.

Argyroudis, S., Kaynia, A.M. and Pitilakis, K. (2013). Development of Fragility Functions for Geotechnical Constructions: Application to Cantilever Retaining Walls. Soil Dynamics and Earthquake Engineering, 50, 106-116. http://dx.doi.org/10.1016/j.soildyn.2013.02.014

Aydan, O., Akagi, T. and Kawamoto, T. (1993). The squeezing potential of rock around tunnels: Theory and prediction, Rock Mechanics and Rock Engineering, Vol. 2, pp. 137–163.

Boydy, E., Bouvand, A. and Pellet, F. (2002). Back analysis of time-dependent behavior of a test gallery in claystone. *Tunnelling and Underground Space Technology,* vol. 17, no. 4. pp. 415-424.

Cabalar, A.F., Cevik, A. and Gokceoglu, C. (2012). Some Applications of Adaptive Neuro-Fuzzy Inference System (ANFIS) in Geotechnical Engineering. Computers and Geotechnics, 40, 14-33.

Charette F. and Plouffe, M. (2008). A new rock bolt concept for underground excavations under high stress conditions. Conferences/GroundSupport2008/225-240.

Hoek, E. (2001). Big tunnels in bad rock (2000 Terzaghi lecture), Journal of Geotechnical and Geo-Environmental Engineering, American Society of Civil Engineers, Vol. 127(9), September 2001, pp. 726–740.

Hoek, E., Kaiser, P.K. and Bawden, W.F. (1995). Support of underground excavations in hard rock, Balkema, Rotterdam.

Gao, Q., Guo, X.L., and Yang, H.T. (2000). GA-based solution for inverse viscoelastic problem. *Journal of Dalian University of Technology,* vol. 40, no. 6. pp. 664-668.

Griggs, D. (1939). Creep of rocks. *Journal of Geology,* vol. 47, no. 8. pp. 225-251.

Jager, A.J. and Ryder, J.A. (1999). A handbook on Rock Engineering Practice for Tabular Hard Rock Mines. Published by The Safety in Mines Research Advisory Committee (SIMRAC).

Jin, F.N. and Pu, K.Y. (1995). Discussion of visco-elastic models. *Chinese Journal of Rock Mechanics and Engineering,* vol. 14, no. 4. pp. 355-361.

Jones, T., Nordlund, E. and Wettainen, T. (2019). Rock Mech Rock Eng. https://doi.org/10.1007/s00603-018-1716-6.
https://link.springer.com/article/10.1007/s00603-018-1716-6

Kellaway, M., Taylor, D. and Keyter, G.J. (2012). The use of geotechnical instrumentation to monitor ground displacements during excavation of the Ingula power caverns, for model calibration and design verification purposes. Braamhoek Consultants Joint Venture. The Southern African Institute of Mining and Metallurgy South African Tunnelling 2012 – Lessons Learnt on Major Projects

Knox, G., Berghorst, A. and Crompton, B. (2018). The relationship between the magnitude of impact velocity per impulse and cumulative absorbed energy capacity of a rock bolt. AusRock 2018: The Fourth Australasian Ground Control in Mining Conference / Sydney, NSW, 28–30 November 2018.

Larsson, K. (2004). Mining Induced Seismicity in Sweden. Licentiate Thesis, Lulea University of Technology.

Liu, X., (1994). Rock Rheological Mechanics Introduction. Geological Press, Beijing.

Liu, B.G. and Sun, J. (1998). Identification of rheological constitutive model of rock mass and its application. *Journal of Northern Jiaotong,* vol. 22, no. 4. pp. 10-14.

Ma, K., Tang, C.A., and Xu, N.W. (2013). Failure precursor of surrounding rock mass around cross tunnel in high-steep rock slop. *Journal of Central South University of Technology,* vol. 20, no. 1. pp. 207-217.

Maghsoudi, A. and Kalantari, B. (2014). Monitoring Instrumentation in Underground Structures. Open Journal of Civil Engineering, 4, 135-146. http://dx.doi.org/10.4236/ojce.2014.42012.

Mercier-Langevin, F. and Turcotte, P. (2007). Evolution of ground support practices at Agnico Eagle's LaRonde Division: innovative solutions to high stress ground. Rock Mechanics: Meeting Society's Challenges and Demands.

Millis, S.W., Chan, E.K.K., Ho, A.N.L., Lau K.W.K. & Sun H.W. (2009). Proceedings of the 17th International Conference on Soil Mechanics and Geotechnical Engineering M. Hamza *et al*. (Eds.) © 2009 IOS Press. doi:10.3233/978-1-60750-031-5-188.

Mostafa, S., Abolfazl, T., and Mohammad, A.M. (2013). Time-dependent behavior of tunnel lining in weak rock mass based on displacement back analysis method. *Tunnelling and Underground Space Technology,* vol. 38. pp. 348-356.

Montassar, S. and de Buhan, P. (2013). Numerical prediction of liquefied ground characteristics from back-analysis of lateral spreading centrifuge experiments. *Computers and Geotechnics,* vol. 52. pp. 7-15.

Moyo, A. (2018). Evaluation of the deformation in the tailrace tunnel of the Ingula Pumped Storage Scheme. MSc. Research report: School of Mining Engineering University of the Witwatersrand Johannesburg, South Africa.

Munson, D.E. (1997). Constitutive model of creep in rock salt applied to underground room closure. *International Journal of Rock Mechanics and Mining Sciences,* vol. 34, no. 2. pp. 233-247.

Nyungu, D. and Stacey, T.R. (2014). Time-dependent tensile strengths of Bushveld Complex rocks and implications for rock failure around mining excavations. *J. S. Afr. Inst. Min. Metall.* [online]. 2014, vol.114, n.10, pp.765-772. ISSN 2411-9717.

Okubo, S., Nishimatsu, Y., and Fukui, K. (1991). Complete creep curves under uniaxial compression. International Journal of Rock Mechanics and Mining Sciences and Geomechanics Abstracts, vol. 28, no. 1. pp. 77-82.

Potvin, Y. and Slade, N. (2007). Controlling extreme ground deformation; Learning from four Australian case studies. Challenges in Deep and High Stress Mining. Y. Potvin, J. Hadjigeorgiou and D. Stacey (eds.), Chapter 40, 2007. pp. 355–361.

Sakurai, S. (2009). Determination of initial stresses and mechanical properties of viscoelastic underground medium. *Proceedings of the 3rd ISRM Congres*s. Colorado University Press, Denver. pp. 1169-1173.

Sandy, M.P., Gibson, W., and Gaudreau, D. (2007). Canadian and Australian ground support practices in high deformation environments. Deep Mining 07, Y. Potvin (ed.). Australian Centre for Geomechanics, 2007. pp. 297–311.

Sikora, Z. and Ossowski, R. (2013). Geotechnical Aspects of Dike Construction Using Soil-Ash Composites. Procedia Engineering, 57, 1029-1035. http://dx.doi.org/10.1016/j.proeng.2013.04.130

Singh, M., Singh, B., and Choudhari, J. (2007). Critical strain and squeezing of rock mass in tunnels. Tunnelling and Underground Space Technology, vol. 22, 2007. pp. 343–350.

Song, Z.P.; Yang, T.T.; Jiang, A.N.; Zhang, D.F.; Jiang, Z.B. (2016). Experimental investigation and numerical simulation of surrounding rock creep for deep mining tunnels. J. S. Afr. Inst. Min. Metall. vol.116 n.12 Johannesburg.

Swart, A.H. and Handley, M.F. (2004). The design of stable stope spans for shallow mining operations. SAIMM Conference, Platinum Adding Value.

Wawersik, W.R. (1974). Time dependent behaviour of rock in compression. *Advances in Rock Mechanics. Proceedings of the 3rd Congress of the International Society of Rock Mechanics,* Colorado. pp. 357-363.

Yao, X.M. (2005). Studying the rock destroy mechanism induced by surrounding rock unloading. Northeastern University, Shenyang.

David Ngonidzashe Nyungu

Business Development Manager CPC & Africa
New Concept Mining

The author started his career with Rio Tinto, Renco Gold Mine graduating to mine planning and mining appointments. He moved to South Africa in 2007 and joined Witwatersrand University where he completed his Master of Science Degree in Mining Engineering. The author joined Middindi Consulting between 2010 and 2011 with whom he acquired enormous surface and underground mining experience. David joined Anglo American Platinum in 2012. He joined AGA's Mponeng Gold Mine as a Senior Rock Engineer in 2016. It was from here that his attention shifted to design and manufacturing of underground support joining new Concept Mining in 2017.

Placement of footwall excavations for an ore replacement project: an underground platinum mining case study

C. Mutsvanga [1] and T Zvarivadza [2]

[1]Sibanye Stillwater – Platinum Division, South Africa
[2]Vimbo Consulting, South Africa

Depletion of mineral resources is a reality of mining. It is critical that as resources get depleted, new reserves are opened up continuously if a mine is to continue operating. In addition to the economic considerations of an ore reserve such as the grade and tonnage, stability of the mining operation is of equal importance. A mine's permanent excavations should remain stable for the period that it remains operational.

The position of footwall excavations in relation to pillars and abutments on the reef horizon determines the stability of these excavations. Because the stresses induced on these excavations can make them prone to instability, they can be several magnitudes higher than the virgin stresses and strength of the rock mass. Methods to determine stress levels and mitigation measures against these stress levels must be determined.

INTRODUCTION

The underground platinum mine in this case study is located within the western Bushveld Complex where platinum bearing reefs are mined. The mine is approximately 5.5 km from the centre of the city of Rustenburg, North West Province, South Africa. Both the Merensky and Upper Group 2 (UG2) reefs are being mined with the middling between the two reefs averaging 140 m.

The current mining area is reaching the mine boundaries, with the Merensky Reef only planned for another 6 – 7 years at current production rates. An ore replacement project (ORP) has been designed to replace the ore reserves that are being depleted on both the Merensky and UG2 reef horizons and also to extend the life of mine (LOM). The UG2 reef is currently being mined from 10 level to level 15 level, (between 400 m and 600 m depth below surface), on both the eastern and western parts of the shaft up to the boundary pillars. The UG2 ORP will range from 16 to 28 levels (600 m to 950 m below surface). The UG2 has not been mined to these depths before and information is limited on excavation stability at these depths.

When the ORP section starts mining, it is important that excavations remain both economically viable and stable for the entire LOM. The excavations should therefore be designed to fulfil these two objectives.

Mining layout

The mine layout has a system of footwall excavations in the form of tunnels and haulages. Haulages are developed at a minimum of 35 m below reef, while crosscuts at the same level are spaced 200 m apart Kuca (2013). See Figure 1 for an illustration of this layout.

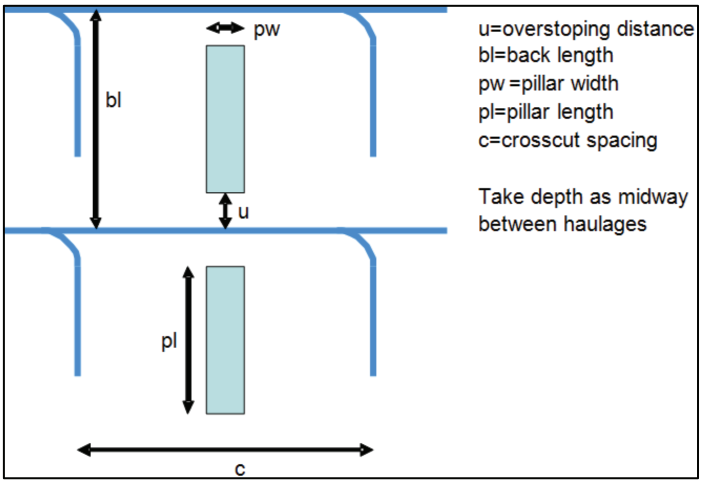

Figure 1. Schematic of the pillar design layout, after Priest (2013)

According to Budavari (1983), service excavations are subjected to stresses and displacement which are induced by the main or productive mining excavations. These effects can be, and often are, severe enough to induce excavation failure and may impact continuity of production. It is clear that the footwall excavations at the platinum mine can be subjected to high field stresses from abutments left on the reef horizon. Thus, it is very important to ensure that when designing regional pillars, the locations of footwall excavations are taken into consideration. A number of strategies to deal with or determine the effect of pillars on footwall excavations are available.

The main objective during the project pillar design was ensuring that the excavations being opened up were not only profitable, but also stable both on and off reef. Rockwall condition factor (RCF) calculations using both empirical and numerical modelling was used to determine the effect of stresses acting on the off-reef excavations and determine whether any mitigating measures would be required. Overstoping is a method that has been successfully used to ensure that the stresses generated due to mining the reef horizon do not adversely affect footwall excavations. Secondary support is an option that can be considered to stabilise excavations where induced stresses are higher than the rock mass strength or are high enough to induce fracturing and therefore potential rock failure. These methods are briefly discussed below.

Rockwall condition factor criterion

A recommended design criterion for expressing and controlling tunnel conditions is the RCF. See Jager and Ryder (1999 a). This criterion is given as:

$$\text{RCF}= \frac{3\sigma_1 - \sigma_3}{F\sigma_c} \qquad [1]$$

Where:

σ_1, σ_3	are the maximum and minimum principal stress components in the plane of the excavation cross section
σ_c	is the uniaxial compressive strength of the host rock
F	is a factor representing the downgrading of σ_c depending on rock mass conditions and excavation size

The formulation of the RCF represents a comparison of the maximum induced tangential stress of an assumed circular excavation to the estimated rock mass strength. It has been found that values of RCF < 0.7 represent good conditions requiring minimum support; 0.7 <RCF < 1.4 average conditions with some robust support and RCF > 1.4 represent poor ground conditions with special support requirements.

OVERSTOPING

Overstoping is when haulages are positioned beneath mined-out areas. According to COMRO (1988 a), consideration should be given to the 45° destressing guideline. An overstoping angle of 45° is generally required to destress haulages. At an angle > 45°, the stress concentrations are high. Figure 2 is a schematic diagram showing how the overstoped zone is determined.

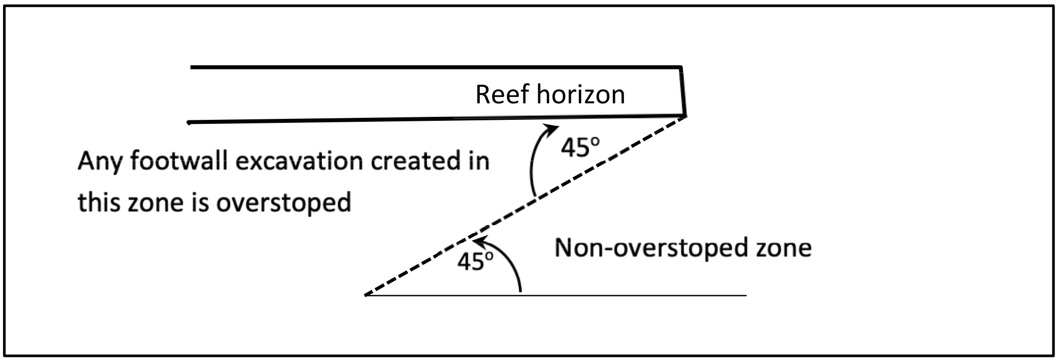

Figure 2. Section diagram showing concept of overstoping.COMRO (1988 b)

NUMERICAL MODELLING

"The RCF concept is empirical and thus may not be ideal for certain conditions," Ryder and Jager, (2002). The overstoping rule "applies only when the section drawn shows a mined-out area that is completely horizontal (dip is 0°). As soon as a reef dip > 0° is shown on the section used to analyse the position of the tunnel, the angle between the reef and the line that separates the *highly stressed* and *de-stressed* zones changes." COMRO (1988 c).

Since the 45-degree rule is crude and based on a specific k-ratio it is therefore prudent to assess the stress conditions with modelling and depending on the k-ratio, this may influence overstoping requirements.

PLACEMENT OF FOOTWALL EXCAVATIONS

Mining depths in KORP section

To determine induced stresses around an excavation it is critical to determine the in situ stresses of the area. The vertical in situ stress magnitude is usually taken as the unit weight of the overlying rock (γ) times the depth (z), Hoek et al (1997). According to a feasibility study, done by Le Bron (2006) the ORP is planned to be mined from 16 to 28 levels. The mining depths for these levels are given in the Table I, based on data from the survey department.

Table I. Mining depths for ORP section

Name	Elevation	Depth below surface (m)
Collar Elevation	**1123.8**	
16 Level	508.2	615.6
19 Level	479.5	644.3
21 Level	422.51	701.3
23 Level	364.7	759.1
25 Level	306.7	817.1
26 Level	277.8	846.0
27 Level	234.5	889.3
28 Level	200.5	923.3

REEF ELEVATION-FOOTWALL EXCAVATION MIDDLING

The middling distances between the reef elevation and footwall excavations, such as crosscuts and haulages, were determined by the survey department based on diamond drilling core drilled for exploration in the ORP section. The range of middling distances for the entire ORP section is given in Table II.

Table II. Reef elevation-footwall excavation middling

Station level	Middling depth range (m)	Comment
16	30.8 – 38.5	Above Reef
19	25.7 – 37.1	Below Reef
21	24.4 – 35.4	Below Reef
23	25.2 – 35.7	Below Reef
25	29.8 – 37.6	Below Reef
26	29.4 – 37.4	Below Reef
27	29.4 – 36.1	Below Reef
28	26.8 – 36.8	Below Reef

As discussed above, footwall excavations such as haulages, crosscuts and chambers may be placed in positions where their stability is not compromised by high induced stresses. It is critical when designing pillars that, they do not generate stresses high enough to cause damage to footwall excavations.

The amount of virgin stresses and/or induced stresses acting on footwall excavations has to be determined, so that a proper support system can be designed for them before instability occurs. Overstoping and the RCF criterion are tools that can be used to ensure that induced stresses from hangingwall abutments on tunnels are managed.

OVERSTOPING

Due to high costs and logistical challenges, it is not always feasible to site footwall excavations sufficiently remote from the reef horizon for them not to be affected by induced stresses. In most cases and for practical purposes, they need to be as close to the reef as possible. A strategy must be developed to deal with the high induced stresses that may develop and affect these excavations. Since it creates a destressed environment early in the stage, overstoping is one way of preventing the footwall excavations from being affected by pillars and abutments created on the reef horizon. Figure 1 (above) shows **u**, the overstoping distance between the edge of the pillar and the haulage. The value of **u** is equivalent to the depth of the excavation below the reef horizon. Figure 2 shows that with **u** equal to the tunnel depth below reef, a 45° angle is created in which the footwall excavations will be in a distressed zone where the stresses created by the abutments do not affect them.

ROCKWALL CONDITION FACTOR

RCF values along the haulages at different depths and levels were calculated using equation 1. Major principal stresses ($\sigma_{1)}$) and minor principal stresses ($\sigma_{3))}$ at these depths were calculated based on stress measurements taken on a neighbouring mine. The stress measurements taken at the neighbouring mine are given in Table III. The footwall excavations occur in pyroxenite rock and the average rock strength ($\sigma_{c)}$) of pyroxenite was derived from UCS tests conducted on core drilled in the ORP section, the value of the rock strength is 166 MPa. The condition factor, F was derived from the average RMR value for the ORP section which was derived during mapping, which is 70, so 0.7 was used as the F value for calculations.

Table IV contains the calculated σ_1, σ_3 and RCF values from 500 m to 1000 m below surface, which is the range of depth below surface for the mining levels in the ORP section as given in Table I.

Table III. Details of the virgin stress tensors, van der Heever and Piper (2013)

Stress component	Magnitude (MPa)	Bearing (degrees)	Dip (degrees)
Sigma 1	42.8	357	32
Sigma 2	28.8	252	22
Sigma 3	24.8	134	50
TauXX (south)	38.1 ± 2.8*		
TauYY (west)	28.0 ± 2.3*		
TauZZ (vertical)	30.4 ± 1.8*		
TauXY	0.2 ± 1.4*		
TauYZ	-1.8 ± 1.1*		
TauZX	7.6 ± 1.4*		
SigHmax	38.1	On bearing 91	
SigHmin	28.0	On bearing 181	
Kmax	1.25	On bearing 91	
kmin	0.92	On bearing 181	
*95% confidence intervals assuming student's t distribution with 7° of freedom			

Table IV. RCF calculations at different depths below surface in the ORP section

Rock density (kg/m3)	**Gravitational force**	**K-ratio**	**Condition factor**	**UCS (MPa)**
2900	9.81	1.25	0.7	166
Depth below surface (m)	σ_1 (MPa)	$3\sigma_1$ (MPa)	σ_3 (MPa)	RCF
500	17.8	53.3	14.2	0.3
550	19.6	58.7	15.6	0.4
600	21.3	64.0	17.1	0.4
650	23.1	69.3	18.5	0.4
700	24.9	74.7	19.9	0.5
750	26.7	80.0	21.3	0.5
800	28.4	85.3	22.8	0.5
850	30.2	90.7	24.2	0.6
900	32.0	96.0	25.6	0.6
950	33.8	101.3	27.0	0.6
1000	35.6	106.7	28.4	0.7

Jager and Ryder (1999 b) gave an empirical relationship between the RCF value, ground conditions of tunnel and support requirements. (See Table V).

Table V. An empirical relationship between the RCF value and the support requirements, Jager and Ryder (1999 c)

RCF Value range	**Ground conditions**	**Support requirements**
< 0.7	Good	Minimum
0.7<RCF<1.4	Average	Moderate
>1.4	Poor	Special

The RCF values calculated for haulages in the ORP section in Table IV are below 0.7 at the different depths. These values indicate good ground conditions and minimal support requirements. This means, no special support to deal with stress induced failures will be required. Further analyses using a numerical modelling program were conducted to determine the influence of mining and pillars left above the excavations, or below in the case of 16 level. The RCF results obtained using a numerical modelling program are given in the section below.

DETERMINATION OF RCF VALUES USING MAP3D PROGRAMME

Introduction

Map3D is a fully integrated 3D layout (CAD), visualisation (GIS) and stability analysis package (BEM stress analysis), MineModelling (2013). Map3D is limited to elastic or elasto-plastic yield behaviour. Being a boundary element solution, the non-linear behaviour is limited to the surface of the elements.

Map3D numerical analyses were conducted to determine the effects of mining and pillars on the reef horizon to the haulages below them. RCF values at different depths below surface were calculated using the empirical equation and all the RCF results obtained indicate good ground condition values of < 0.7 (See Table IV). These results were based on in situ stress conditions. To determine the effects of induced stresses on tunnels and haulages requires numerical modelling analysis. Map3D due to its 3D capabilities was the numerical modelling programme chosen for the analyses. A model was constructed on the excavation and grid lines placed along the haulages that have been mined or are planned to be mined. A numerical model analysis was then run along this grid to determine the RCF values to be expected. The most essential aspect was to analyse the influence of the regional pillars both below in the case of 16 level haulages and above in the case of all the other levels.

The parameters that were used in the numerical model analyses for RCF determination are:

F = 0.7 (based on the RMR value of the ORP section)
σ_c = 166 MPa (the UCS value for pyroxenite rock where the footwall excavations will be situated).

Ideally RCF values of less than 0.7 are desired, but with additional support installed values of up to 1.3 can be managed. RCF values of more than 1.4 should be avoided and values above 2 will indicate to a potential loss of the excavation.

Figure 3 to Figure 6 are images and graphs of the RCF values obtained along the length of the excavations on each level based on the designed pillars and mining layout. The spike in values on each graph; represent the portion where the excavation passes within a regional pillar.

16 level RCF values

Figure 3 is an image of the model of RCF analysis on the return airway (RAW) and haulage at 16 level which is mined above the 19 level stoping elevation. The model results are represented graphically in Figures 4. The graph shows RCF values spiking in positions where the haulages are directly above the regional pillars. The RCF values of the haulage peak at 1.8, whilst those of the RAW peaks at 2.0. The RCF values along the rest of the excavations have values below 0.5. This indicates that the pillars will have a direct influence on the excavations above and will induce high stresses that have the potential to cause failure in the haulage and RAW. Therefore, there is potential for very poor ground conditions at positions just above the pillars and good conditions along the rest of the excavations. The solution to mitigate potential instability is either to install robust support where the excavations are above the pillars or to break up the pillar over the excavations so as to overstope them. However, as can be seen in Figure 3 if the pillar is broken up a very small pillar will be left on the right side of the image and numerical modelling analyses will be required to determine the effect of this on the RCF values of the haulages, and on the average pillar stress (APS) of the pillars themselves and ensuring that they continue to meet the design criteria.

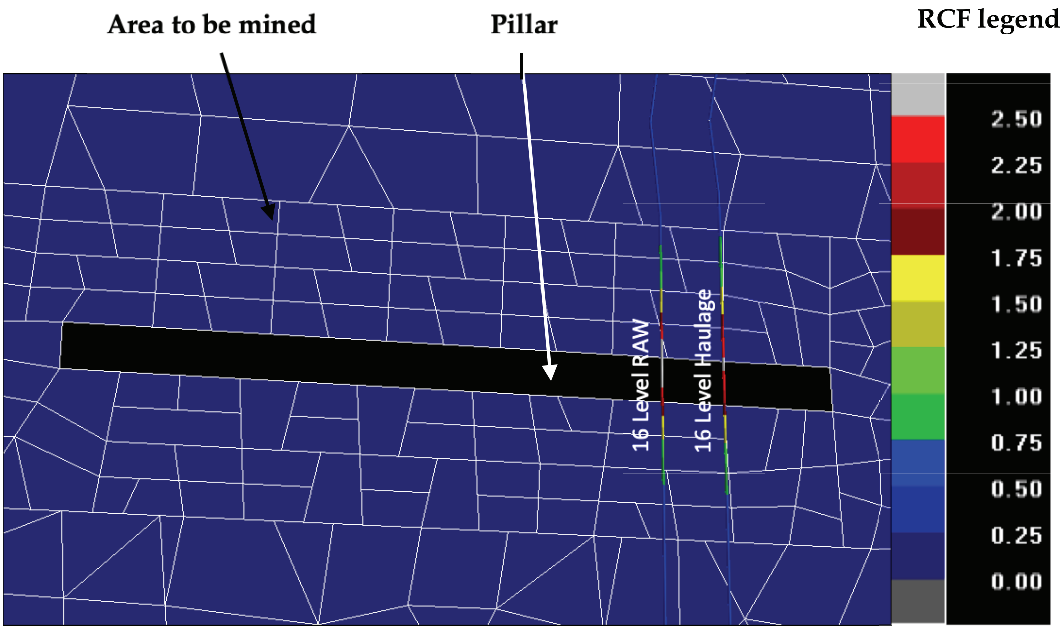

Figure 3. A Map3D model of the RAW and haulage at 16 level running above 19 level (Note the high RCF values on the pillar position)

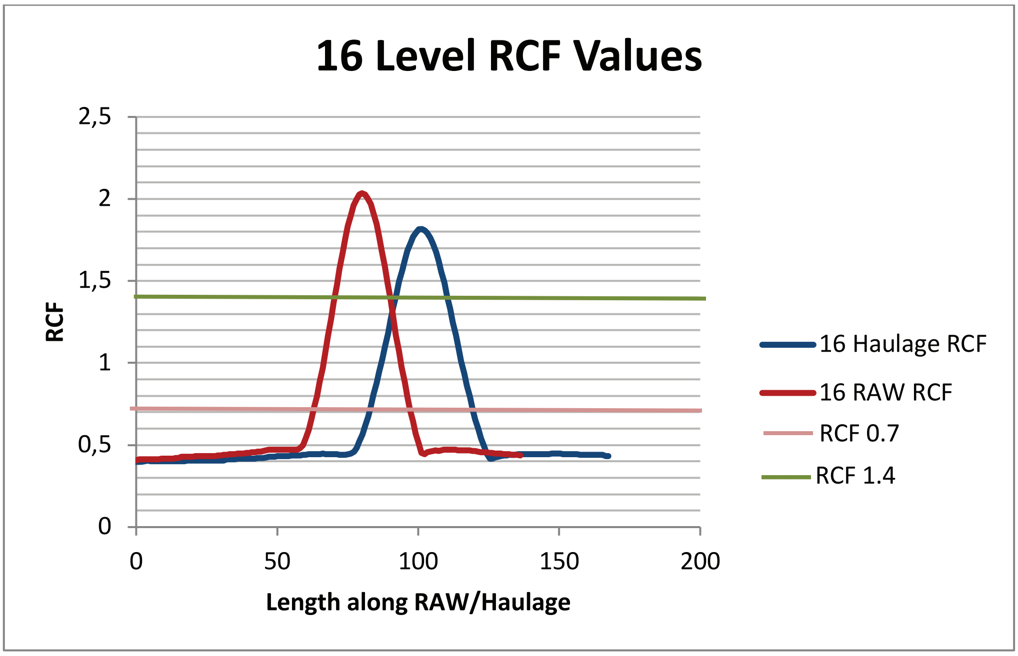

Figure 4. Graphical representation of the RCF values modelled along the haulage and RAW on 16 level mined above 19 level stoping

19 - 28 level RCF values

Level 19 to 28 haulages are all situated below their respective stoping levels and were designed to be overstoped, meaning there is no pillar directly above the haulage, and that the 45º rule was applied. As can be seen in Figure 5, level 25, has a portion along its length with RCF value >1. Figure 6 is a graph showing RCF values along the different haulages at different depths below surface levels.

All the haulages, except those on 25 level, have RCF values which indicate stability as they are all below 1. At 25 level, some rehabilitation work may be required where the RCF values are >1. An alternative to alleviate this problem would be to reduce pillar lengths so as to increase the overstoping distances, then doing numerical modelling analysis on the shortened pillars to determine the new RCF and APS values.

RCF legend

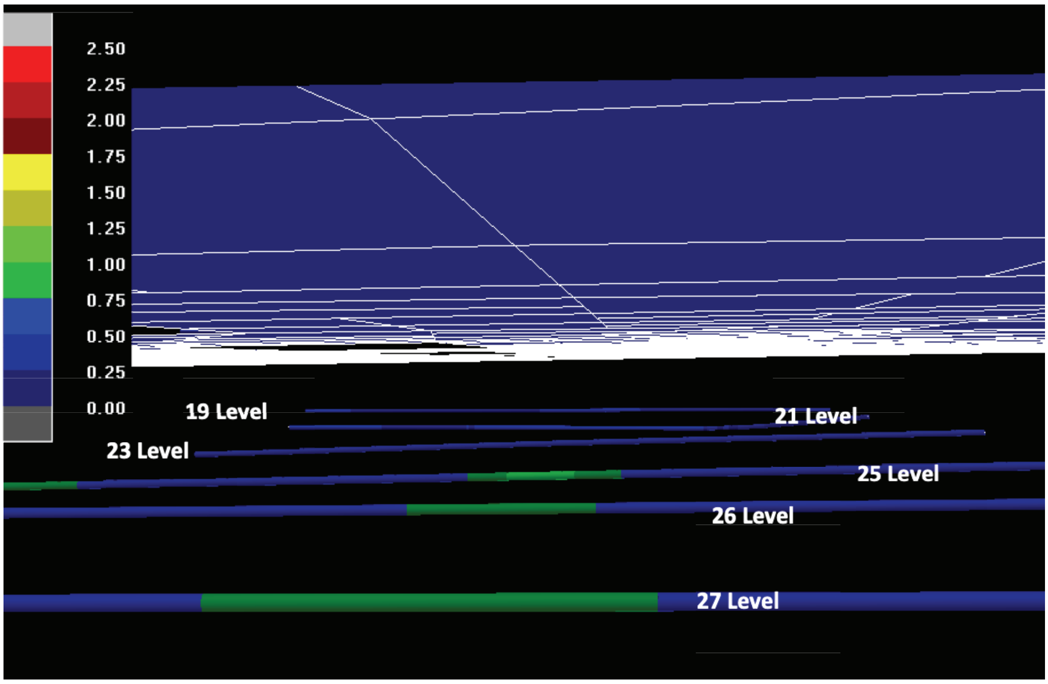

Figure 5. A Map3D model of the 19 to 27 level haulages running below their respective levels (There is no noticeable spike in RCF values)

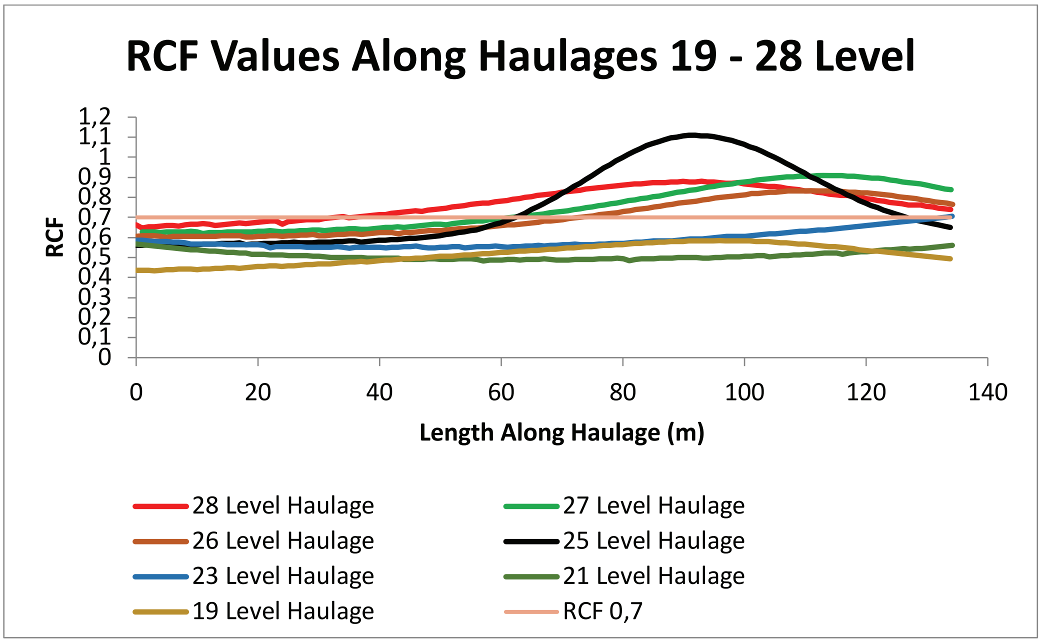

Figure 6. Graphical representation of the RCF values modelled along the haulages from 19 to 28 levels

CONCLUSIONS

The effects of mining and regional pillars on footwall excavations was analysed using empirical and numerical modelling methods for the ORP at the underground platinum mine. RCF values determined empirically indicated stable conditions in the excavations.

Through numerical modelling, 16 level haulages which are mining above 19 level stoping, have indicated RCF values of up to 2. This value represents poor ground conditions requiring a robust support system. An alternative would be to understope the haulages but this would require proper analysis.

Due to the overstoping of the haulages from 19 to 28 levels, the RCF values are significantly low enough to warrant any further action being taken in terms of support, with the exception of monitoring to validate the results. Most of the RCF values are below 0.7 which are good ground conditions values with maximum values slightly above 1 at 25 level. It will be critical to ensure that no pillars or abutments are left above the haulages as this has the potential to induce stresses that are higher than the rock strength thereby causing excavation failure.

It is essential to establish a monitoring programme to determine whether any deformation is occurring in the haulages once mining commences, to validate the modelling results and re-evaluate the support strategy where necessary.

REFERENCES

Budavari, S. (1983). Rock Mechanics in Mining Practice. Johannesburg: SAIMM.

COMRO (1988). Industry Guide to Methods of Ameliorating the Hazards of Rockfalls and Rockbursts. Johannesburg: Chamber of Mines.

Hoek, E., Kaiser, P. and Bawden, W. (1997). Support of Underground Excavations in Hard Rock. 2nd ed. Rotterdam: A.A. Balkema.

Jager, A. and Ryder, J. (1999). a handbook on Rock Engineering Practice for tabular hardrock mines. Johannesburg: SIMRAC.

Kuca, J. (2013). Group Procedure: Crosscut, raise development and ledging, Johannesburg: Anglo American Platinum.

Le Bron, K. (2006). Townlands Ore Replacement Project Feasibility Study Geotechnical, Rustenburg: Anglo Platinum.

MineModelling, P. (2013). Map3D User's Manual. Victoria, Australia: Mine Modelling Pty Ltd

Priest, G. (2013). Regional Support, Johannesburg: Anglo American Platinum.

Ryder, J. A. and Jager, A. (2002). A Text Book on Rock Mechanics for Tabular Hard Rock Mines. 1st ed. Johannesburg: SIMRAC.

Van der Heever, P. and Piper, P. (2013). In-situ Stress Measurements on 34 Level, Siphumelele Shaft, Rustenburg Section, Johannesburg: Groundwork.

Clarence Mutsvanga

Unit Manager Rock Engineering,
banye Stillwater

2017 – Present	Unit Manager Rock Engineering, Sibanye Stillwater – Platinum Division, Rustenburg
2016 – 2017	(Anglo takeover) Shaft Rock Engineer, Sibanye Stillwater – Platinum Division, Rustenburg
2012 – 2016	Shaft Rock Engineer, Anglo American Platinum, Rustenburg
2011 – 2011	Strata control officer Open House Management Solutions, Two Rivers Platinum Mines
2007 – 2010	Strata control officer Unki mine, Zimbabwe

The Polihali diversion tunnels: A case study on the design of tunnels in Lesotho basalts

C. Warren-Codrington[1] and G. J. Keyter[2]

[1]MSKC (a Joint Venture of Aurecon South Africa, Hatch Africa, Knight Piésold, SMEC South Africa & FM Associates)
[2]SRK Consulting South Africa

Phase II of the Lesotho Highlands Water Project (LHWP) expands on the successful completion of Phase I in 2003. A cornerstone of the water transfer component of Phase II is Polihali Dam, a concrete faced rockfill dam (CFRD) with a height of 163.5 m, which will augment water supply to Katse Dam through the approximately 38 km long Polihali transfer tunnel. This paper focuses on the design of rock support for the Polihali diversion tunnels which will be constructed on the left flank of the Senqu River at the site of Polihali Dam. Firstly, the interpretation of geotechnical investigation data and its assimilation into the design of the diversion tunnels is described. This includes consideration for the durability of different Lesotho Formation basalt flows, structural characteristics, rock mass permeability, variable rock mass strength and deformation characteristics. Secondly, the use of empirical methods combined with finite element method (FEM) computational modelling to design tunnel rock support for different rock mass conditions is described. Consideration was given to rock-support interactions to ensure an efficient and safe support installation sequence.

INTRODUCTION

The Lesotho Highlands Water Project (LHWP) is an ongoing water supply and hydropower generation project which continues to have an important impact on the infrastructure and economic development of Lesotho and South Africa. Phase II, which builds on the successful completion of Phases IA and IB, is currently underway. A cornerstone of Phase II is the 163.5 m high Polihali concrete faced rockfill dam (CFRD) to be built at the confluence of the Senqu and Khubelu rivers. Phase II will augment water supply to Katse Dam through the approximately 38 km long Polihali transfer tunnel. In doing so, it will play a central role in supporting the economic growth and development of Lesotho and South Africa for decades to come.

Advanced work for the Polihali Dam and transfer tunnel commenced in 2018 with construction of the Polihali north east access road (PNEAR) and the construction of Polihali Village, as well as construction camps and associated infrastructure at Masokong Village, near Mokhotlong. In due course the construction of an operations centre, roads and bridges, telecommunication networks, sewage and water treatment works, clinics and lodges will be undertaken within a framework of proactive environmental and social development measures to ensure efficient and sustainable benefits.

Essential to the construction of the Polihali Dam are the Polihali diversion tunnels which were designed in 2017 by the Metsi a Senqu-Khubelu Consultants joint venture (MSKC JV). Construction of the diversion tunnels is set to commence in 2019 and will last approximately 18 months. These comprise two parallel D-shaped tunnels, one with a 7 m span (DT1) and the other with a 9 m (DT2) span, each approximately 1 km long and designed to divert water from the Senqu and Khubelu rivers during the construction of the Polihali Dam.

Salient features of the diversion tunnel design are described in this paper. Aspects regarding rock mass classification and characterisation are addressed first, followed by a summary of the empirical tunnel support classification tools used. The use of support capacity diagrams as a tool to verify and optimise the estimated rock support is then described.

The principal objective is to demonstrate a rational tunnel design methodology using a combination of empirical and 2D numerical modelling tools while highlighting key design aspects of water conveying tunnels in basaltic rock.

Specifics of the geotechnical investigations, design of the tunnel approach excavations, rock fall protection measures, tunnel hydraulic and hydrofracturing assessments, tunnel portal support and the contractual aspects of the tunnel design and construction, although essential to the design of the diversion tunnels, fall outside the scope of this paper.

GEOLOGICAL SETTING

Regional geology

The Polihali Dam site is located entirely within the basalt lavas of the Lesotho Formation/Drakensberg Group. The outpouring of the basalts appears to have started in Upper Triassic times (about 190 million years ago) and cut short the deposition of the underlying windblown Clarens Formation sandstone. Basalt has been extruded flow upon flow to a thickness of at least 1 400 m.

The basalt flows appear to have cooled relatively rapidly following extrusion to produce small to very small crystals of plagioclase, feldspar and pyroxene with subsidiary olivine set in a groundmass of chilled volcanic glass. Four main types of basalt are recognised and may be classified depending on the proportion of amygdales as follows: (1) basalts without amygdales, of which doleritic basalts (DB) and non-amygdaloidal basalts (NAB) with or without disseminated soft spots (DSS) are distinguished, and; (2) basalts with amygdales, comprising either highly amygdaloidal basalts (HAB) with greater than 10% amygdales, or moderately amygdaloidal basalts (MAB) which contain between 1% and 10% amygdales.

Basalt durability

Durability issues are known to be associated with the Lesotho basalts. Of the types of basalt encountered, the doleritic variety with low olivine content appears to be the most durable. Of slightly lesser durability are the varieties of basalt with low proportions of DSS, calcite or quartz as the only amygdale fill, and very limited content of swelling clays or laumontite either as amygdale fill or in the groundmass. Doleritic basalt with a high proportion of olivine, non-amygdaloidal basalt with a high proportion of DSS and amygdaloidal basalts with a high content of clay in the filling of amygdales appear to be the least durable.

Earlier investigations of unlined tunnels in Lesotho basalts appeared to indicate that, at relatively shallow depth, most basalts remain stable. Only those with the more extreme content of laumontite, olivine, and swelling clays seem to require protection to prevent ongoing deterioration in such environments.

That said, analyses on core samples revealed that all three basalt types (NAB, MAB and HAB) in the project area contain in the order of 18% to 20% smectite, while HAB also contained some 14% laumontite. It was concluded that such basalts are likely non-durable and would require mitigating measures to be incorporated in the design of tunnel support. Fundamental to the design of rock support and tunnel linings was determining the relative proportions of these minerals within each basalt flow and especially the tunnel zone.

In situ stress state
In lieu of site-specific in situ stress data, a horizontal to vertical stress ratio (K-ratio) of 1.0 was initially assumed. This was varied between 0.5 and 1.5 in subsequent analyses to evaluate the sensitivity of the support design to variations in in situ stress.

DESIGN APPROACH

Design basis and methodology
The design basis for the Polihali diversion tunnels was rooted in the New Austrian Tunnelling Method (NATM), assuming conventional drill-and-blast techniques. A working stress approach was adopted for the design of the diversion tunnels in accordance with Hoek et al (1993). Rock support in tunnel excavations was designed as permanent support, with an adequate level of corrosion protection provided to ensure the long-term functionality of all the support elements installed.

Methods of analysis used in the design of underground excavations during diversion tunnel construction, included assessment of the potential for structurally controlled instability and the use of empirical methods of support selection and design based on precedent experience using Barton's Q-System (Barton et al (1974); Barton et al (1993); Barton (2002). This was followed by convergence confinement methods and 2D FEM numerical analyses.

Standards, guidelines and acceptance criteria
A minimum factor of safety of 1.5 was adopted for the design of rockbolts in accordance with Hoek et al (1993). Shotcrete elements were designed such that a factor of safety of 2.0 was achieved for permanent loads and 1.5 for temporary or variable loads Hoek et al (2008).

The tunnel design was furthermore carried out in accordance with guidelines published by SANCOT (1992), BTS/ICE (2000) and the ITA, with cognisance also taken of requirements specified by BS 8081:1981.

Tunnel alignment, cross-section and cover considerations
DT1 and DT2 were designed with a D-shaped cross-section and finished spans of 7 m and 9 m, respectively. However, over the first 35 m of tunnel, the spans of DT1 and DT2 were increased to 9 m and 11 m, respectively, to accommodate the cast in-situ concrete lined section of tunnel at the intake structures.

A minimum ground cover of two tunnel spans in competent rock was adopted in designing the horizontal and vertical alignment of the diversion tunnels USACE (1999). The highest ground cover of 115 m resulted in a maximum lithostatic stress of 3.2 MPa at tunnel level. Consequently, the in-situ stress at tunnel level was anticipated to be well below the intact strength of the rock and stress-induced instability in the form of rock spalling was thus not considered likely.

STRUCTURALLY CONTROLLED INSTABILITY

Joint orientations
Joint orientation measurements from oriented borehole cores were plotted on equal area lower hemisphere stereonets. An example of such a stereonet is included in Figure 1. The main joint sets were identified based on contouring of the joint data. Sub-horizontal flow contacts between the different basalt flows have been excluded from these diagrams, and Joint Set JS1a appears to be a subset of Joint Set 1.

It was concluded that two main joint sets would be present: steeply dipping joints that either strike NS or WE, in addition to sub-horizontal flow contacts. Random joints were also expected as there is considerable scatter in the data collected.

Rock mass permeability
Lugeon tests undertaken in boreholes within the tunnel corridor indicated tight jointing. Typically, only negligible water loss was recorded; however, occasional, isolated significant losses were recorded. The permeability of the basalts was therefore deemed to be low, with water seepage expected to be limited to a few open joints that occur at random, and more commonly near vertical lineaments and dykes.

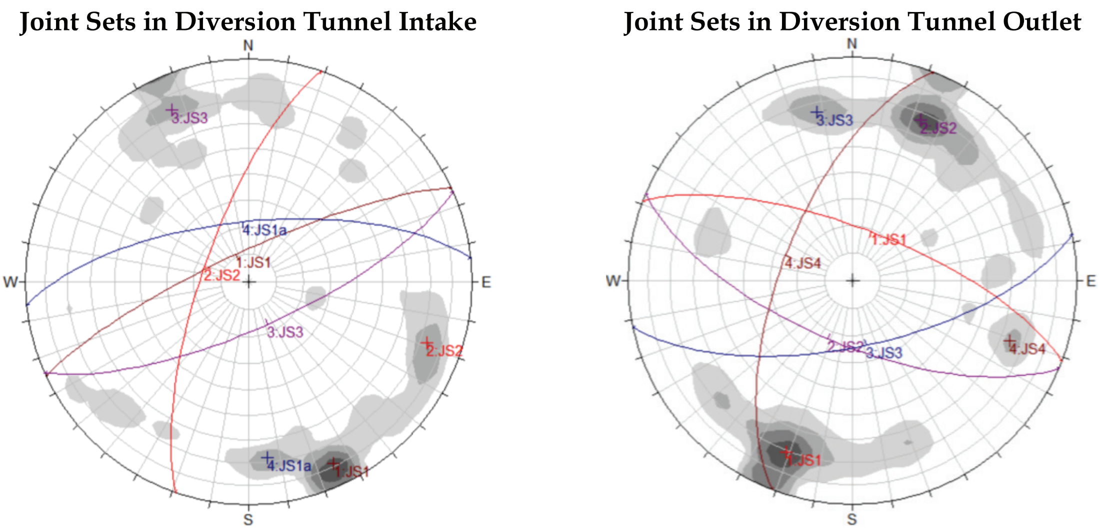

Figure 1. Joint sets in diversion tunnel intake and outlet areas

Joint persistence
Observations made in surface erosion gulleys during field mapping noted jointing was typically not cross-cutting between respective basalt flows but instead, appeared to be confined within individual flows. In the diversion tunnel intake area, the thickness of individual flows averaged 1.4 m to 2.8 m. In the diversion tunnel outlet area, the thickness of individual flows averaged 1.1 m to 5.9 m. Other individual flows noted within the diversion tunnel corridor had an average thickness of 4.3 m to 4.5 m. Therefore, with joints confined within individual flows as noted above, it was concluded that joint persistence could generally be assumed to be of the order of 10 m or less.

Joint shear strength
An estimate of the shear strength of joints in the basalts was based on typical joint descriptions in the borehole logs. The joints were generally described as rough, non-planar with asperities of less than 5 mm. In slightly weathered to unweathered rock at depth, the joint wall hardness was described as hard and cannot be scratched with a steel knife. In the slightly weathered to unweathered rock mass, joint infill was either absent, or where present, generally comprised calcite.

From this basic friction angles (φ_{b}) of 31 (wet) and 38 degrees (dry) were estimated based on laboratory tests on saw-cut samples of intact basalt rock, Stacey et al (1986). Note that φ_b was increased by 6^{o} to account for roughness -rough, with defined ridges/asperities. This resulted in an estimated joint friction angle in the order of 37 for the slightly weathered to unweathered basalts in wet conditions.

Assessment of structurally controlled instability
Overbreak was considered inevitable in the unsupported face area of the tunnel due to the tunnel dimensions and its intersection with sub-horizontal flow contacts coupled with the two main joint sets. To mitigate the risk of structurally controlled instability, firstly, the maximum unsupported span between the last line of initial support installed and the tunnel face was controlled by specifying a maximum round length for the different support classes. Secondly, controlled perimeter drilling and blasting techniques were specified to reduce blast induced damage in the excavated tunnel perimeter.

Furthermore, routine geological mapping was specified in the tunnel face area after every blast, with the aim of identifying flow contacts and jointing in the face area, so that larger, potentially unstable rock wedges can be timeously identified to allow installation of rock support as may be appropriate.

This notwithstanding, based on the favourable discontinuity orientation and persistence, coupled with the relatively high estimated joint shear strength, it was concluded that the rock mass response to excavation could be simulated with sufficient accuracy by treating the rock mass as a continuum.

ROCK MASS CHARACTERISATION

Rock mass classification studies

Barton's Q-System classification and support chart Barton et al (1974; Barton et al (1993; Barton (2002) , was the primary method used to estimate rock support required for the range of ground conditions expected. Barton et al (1974) defined the tunnelling quality index Q in Equation (1) as follows:

$$Q = \frac{RQD}{J_n} \cdot \frac{J_r}{J_a} \cdot \frac{J_w}{SRF} \qquad [1]$$

RQD, J_n, J_r, J_a respectively denote the rock quality designation, joint number, joint roughness and joint alteration. J_w denotes the joint water reduction factor and SRF denotes the stress reduction factor.

Figure 2 and Figure 3 illustrate the frequency distribution for each of the Q-System parameters from boreholes drilled within the diversion tunnel corridor. Assuming a J_w = 0.66 (medium inflow or groundwater pressure) and an SRF = 1.0 (medium in-situ ground stresses) a representative Q-value range of 0.8 to 13 was determined. Therefore, the slightly weathered to unweathered basalts generally fell within the "fair" to "good" rock mass category with 4 < Q < 10. Corresponding rock mass classification studies based on the rock mass rating (RMR) and rock mass index (RMi) systems (Palmström, 2009) gave 60 < RMR < 70 and 2.5 < RMi < 9, respectively. Three Support Classes were therefore defined as follows - Class I: Q > 10, Class II 4 < Q ≤10 and Class III: 0.8 ≤ Q ≤ 4.

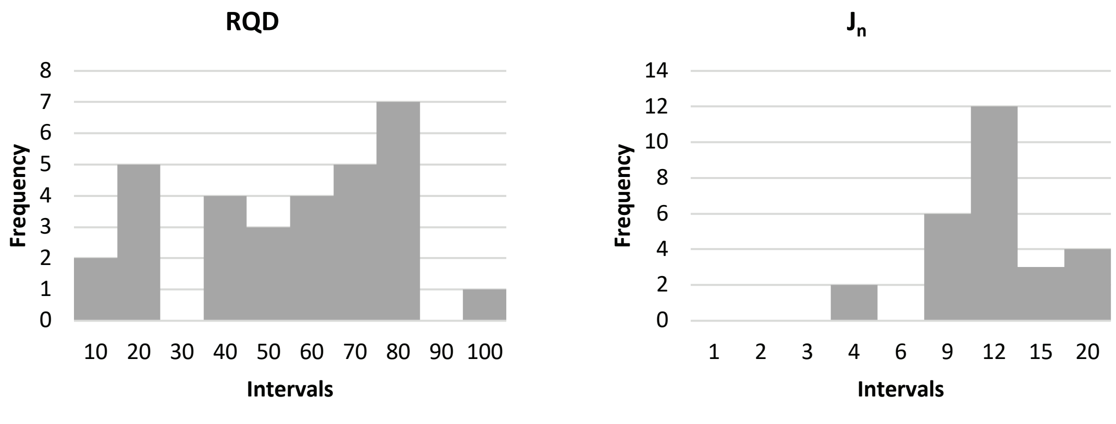

Figure 2. RQD and J_n are a measure of relative block size

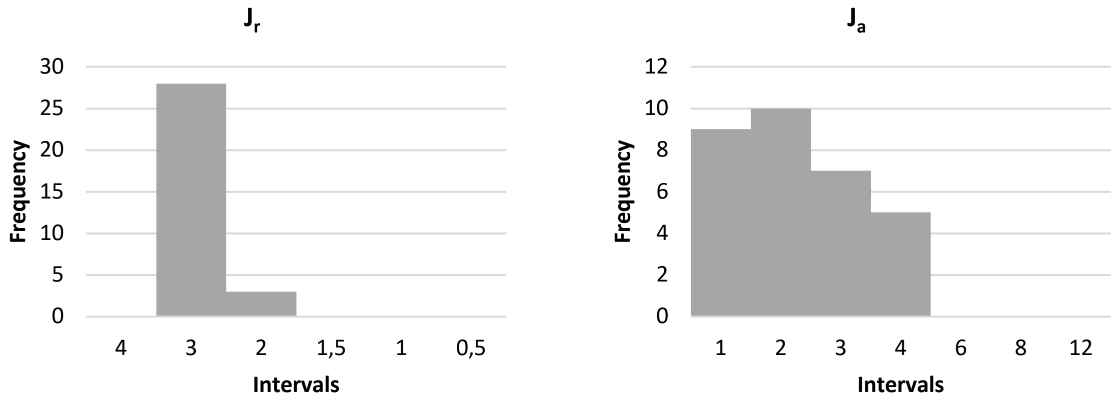

Figure 3. J_r and J_a are a measure of joint roughness and frictional characteristics of joint walls/infill

Intact rock strength and deformation properties

Laboratory tests comprising uniaxial compressive strength with strain measurement (UCS, UCM), triaxial compressive strength tests (TCS) and Young's modulus (E) were carried out on representative intact rock core specimens from boreholes drilled within the diversion tunnel corridor.

The intact rock properties adopted for modelling and design of Class I to Class III based on the above review are presented in Table I. Figure 4 presents the range and quartiles of the available UCS and tangent modulus (E_i) test results. Characteristic values were defined as the lower limit of the 95% confidence interval for the population mean. Plotted alongside the characteristic values indicated are the designated UCS and E design values for Classes I to III as defined above.

Table I. Intact rock properties in different support classes

Support class	Q-Value	UCS (MPa)	E_i (GPa)
I	>10	175 (150 – 200)	35.0 (35.0 – 61.3)
I	4-10	125 (100 – 150)	30.0 (26.3 – 43.8)
III	0.8-4	50 (50 – 100)	17.5 (12.5 – 35.0)

Rock mass strength and deformation properties

The Q-value ranges, based on which the various support classes were derived, and corresponding intact properties were used to define rock mass strengths for the different support classes using the Generalized Hoek-Brown failure criterion Hoek et al (2002). This criterion was chosen, firstly, for its ability to accurately predict the non-linearity of shear stress over a wide range of confining stresses; secondly, it is an empirical formulation developed from extensive laboratory and in-situ test data; and, thirdly, it provides a straight forward means of deriving rock mass properties when discontinuity networks do not govern the behaviour of the rock mass.

The geological strength index (GSI) values used to calculate rock mass strengths for the different support classes were based on Equation [2] Hoek et al (1995). Rock mass moduli (E_{rm}) for the different support classes were derived using Equation [3] Hoek et al (2006). The resultant rock mass strength (σ_{cm}) and deformation moduli (E_{rm}) derived for support classes I to III and used in subsequent FEM simulations are presented in Table II.

$$GSI = 9\ln(Q') + 44, \text{ where } Q' = Q \cdot \frac{SRF}{J_w} \qquad [2]$$

$$E_{rm} = E_i \cdot \left(0.02 + \frac{1 - {}^{D}\!/_{2}}{1 + e^{\left(\frac{60 + 15D - GSI}{11}\right)}} \right) \qquad [3]$$

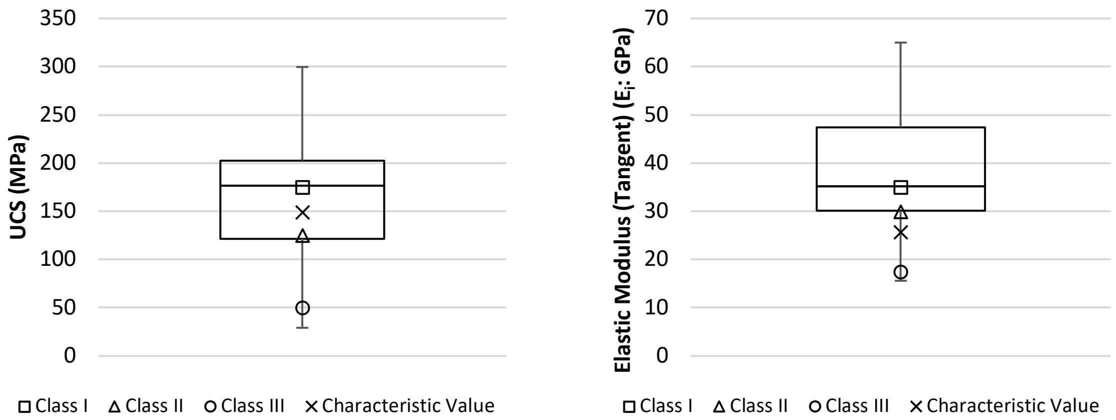

Figure 4. Statistical summary of uniaxial compressive strength (UCS) and intact elastic moduli (E_i)

Table II. Rock mass strength and deformation moduli in different support classes

Support class	Q'	GSI	σ_{cm} (MPa)	E_{rm} (GPa)
I	> 15	70 (60 – 70)	72	25.6
II	6 – 15	60 (50 – 60)	41	15.6
II	1.2 – 6	45 (40 – 50)	12	5.0

The ratio of in situ stress (p_0) to rock mass strength (σ_{cm}) exceeds 0.2 for all three support classes. Based on precedent experience, this indicates a low potential for stress-related instability/spalling and instability of the tunnel face (Hoek (1998). Consequently, limiting the plastic radial strain of the tunnel to prevent face instability was not considered necessary.

ROCK SUPPORT CLASSIFICATION AND ANALYSIS

Empirical rock support classification

An empirical estimate of rock support was made based on the rock mass classifications described in Section 4. To simplify construction, the rock support was standardised between DT1 and DT2. The estimated support is summarised in Table III. A minimum shotcrete thickness of 50 mm was specified to mitigate the risk posed by rapidly deteriorating basalt.

Table III. Summary of rock support in different support classes

Class	Span for DT1 & (DT2)	Maximum round length	Tunnel support
I	7.4 (9.4)	5 m	3.5 m long, 25 mm dia. rockbolts; 50 mm shotcrete
II	7.4 (9.4)	4 m	3.5 m long, 25 mm dia. rockbolts; 50 mm shotcrete
III	7.5 (9.5)	3 m	3.5 m long, 25 mm dia. rockbolts; 100 mm shotcrete

Convergence confinement analyses
A 2D plane strain convergence confinement analysis was carried out for the diversion tunnels using Phase2 FEM software developed by Rocscience. This assessed the ground response to excavation and its interaction with installed support assuming the rock mass to be a continuum.

The excavation dimensions and stress conditions relevant to Support Class III were used as these were considered the critical design scenario for ground conditions expected in diversion tunnel excavations.

The pressure reduction method was used to derive the characteristic response curve for each diversion tunnel. Accordingly, the diversion tunnels were converted to equivalent circular tunnels as per the recommendations by Curran et al (2002). Table IV summarises the tunnel dimensions and in-situ stress state assumed for these convergence confinement analyses.

Table IV. Input parameters for convergence confinement analysis

Parameter	DT1	DT2
Tunnel excavated span	7.52 m	9.53 m
Cross-sectional area	48 m^2	77.9 m^2
Equivalent tunnel radius	3.9 m	5.0 m
In situ vertical stress (p_0)	3.2 MPa	
Stress ratio (K)	1.0	

Figure 5 presents the characteristic curves and longitudinal displacement profile for the diversion tunnels. The formulation proposed by Vlachopoulos et al (2009) was used to estimate the longitudinal displacement profile.

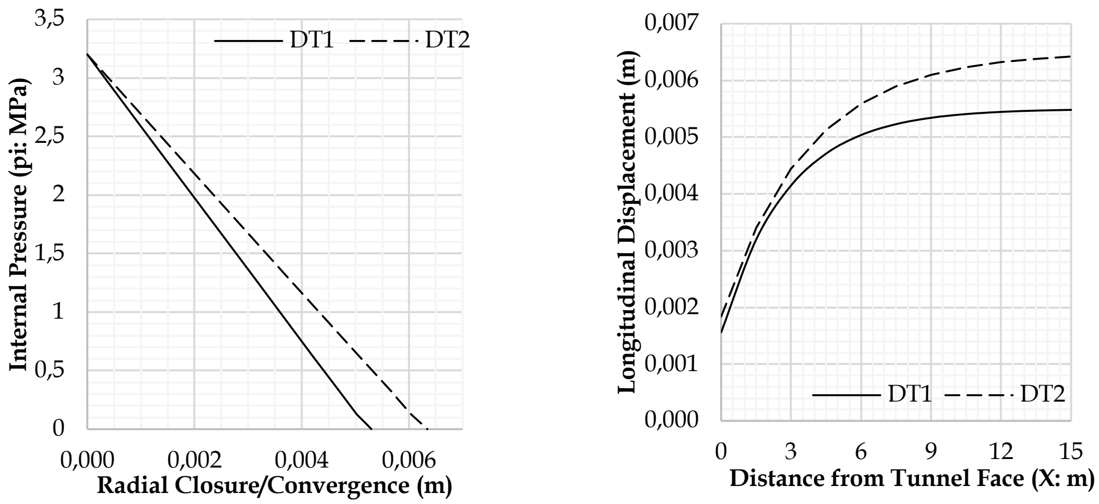

Figure 5. Ground reaction/characteristic curves and longitudinal displacement profile

These analyses indicated a plastic zone , an overstressed rock zone, around the tunnel periphery with a thickness of between 0.3 m and 1.2 m, based on which it was concluded that the 3.5 m long rockbolts specified from the empirical method is adequate considering guidelines by Hoek (1998, 2001) to ensure a rockbolt bonded length of at least 1.5 m into undisturbed rock.

Furthermore, with reference to the results presented in Figure 5, rockbolts installed at the face (i.e. at X = 0 m) before blasting the next round would extend approximately 5 mm due to tunnel crown/sidewall convergence. The load induced by such extension would be close to the limit of the rockbolt's acceptable working load. Installation of rockbolts 1 m to 2 m from the tunnel face before blasting the next round, would result in lesser extension of the rockbolts, resulting in a lower working load in the bolt. Subsequent numerical modelling in tunnel excavation and support analyses compared tunnel support installed at X = 1.5 m from the tunnel face for Class III with support installed up to the tunnel face, i.e. at X = 0 m.

TUNNEL EXCAVATION AND SUPPORT ANALYSIS

Excavation-support sequence modelling

2D Phase2 FEM convergence confinement models were developed to model the tunnel excavation and support specified in more detail. The tunnel advance was simulated by incrementally reducing the ratio of internal pressure to in-situ stress (p_i/p_0). The internal pressure ratio at which the support was installed was varied from what corresponded to installing support a distance of 0 m to 1.5 m from the tunnel face Vlachopoulos et al (2009). The aim of this was to establish a safe and optimal support installation strategy.

Table V presents the Phase2 FEM stages used to model the sequence of tunnel excavation and support installation for a scenario where support was assumed to be installed 1.5 m from the tunnel face. This analysis incorporated the time dependent development of sprayed concrete strength and stiffness concurrent with the advancing tunnel face, as discussed below.

Tunnel support properties

The properties of rock support elements used in the Phase2 FEM models are summarized in Table VI and Table VII. Mechanically end anchored, fully cement grouted rockbolts were modelled as end-anchored bolts in Phase2. The time-dependent properties of the reinforced sprayed concrete as a function of its 28 day strength and modulus parameters were defined according to CEB-FIP Model Code (1990) and Schutz (2010).

Evaluation of support capacity

Support capacity diagrams based on elastic analyses as proposed by Hoek et al (2008) were used to evaluate the capacity of each support element and, in doing so, evaluate the appropriateness of the support sequence adopted following the empirically based tunnel support estimates described earlier.

Table V. Stages used to model sequence of tunnel excavation and support

Stage		p_i/p_0	Description
1	In situ	1.00	In situ stress state
2	Tunnel relaxation	0.47	Simulate respective tunnel closure up to a distance X = 1.5 m behind the tunnel face.
3	Initial support installation	0.47	Install initial support rockbolts and weld mesh reinforced sprayed concrete.
4	12 hours	0.21	
5	36 hours	0.09	Sprayed concrete strength and modulus increase as the tunnel face advances, assuming typical blast-to-blast cycle times of 24 hours.
6	60 hours	0.04	
7	84 hours	0.01	
8	28 days	0.00	

Table VI. Rockbolt properties

Parameter	Design Value
Steel modulus (E)	200 GPa
Characteristic strength (f_y)	450 MPa
Tensile capacity (T_b)	221 kN
Pre-tension (T_p)	100 kN

Table VII. Mesh reinforced sprayed concrete properties

Parameter	Design value
Young's modulus (E_c)	26 GPa (at 28 days)
Poisson's ratio (υ)	0.15
Compressive strength (f_c)	35 MPa (at 28 days)
Tensile strength	3 MPa (at 28 days)

Figure 6 illustrates the axial force-moment capacity diagram for the reinforced sprayed concrete at an age of 12 hours, i.e., when the next blast cycle was assumed to take place. This showed tensile cracking and/or compressive crushing of the shotcrete when installed up to the tunnel face. No cracking of the shotcrete was noted with the shotcrete installed up to 1.5 m from the tunnel face.

Figure 7 shows the final tunnel profile for DT2 at 28 days following support installation. A maximum rockbolt axial force of 165 kN was noted when installed up to the tunnel face. This reduced to 150 kN if rockbolts were installed 1.5 m from the tunnel face.

These results confirmed findings from the earlier convergence-confinement analyses, based on which it was decided that rockbolts should typically be installed to within a distance of 1.5 m to 2 m from the tunnel face to reduce the risk of support becoming overstressed.

DESIGN & CONSTRUCTION DETAILS

The preceding support capacity simulations confirmed that conventional drill and blast techniques provided an acceptable means of diversion tunnel construction. The use of appropriately sized multi-boom face drilling rigs were anticipated. Furthermore, excavation of the diversion tunnels using a single full-face heading was shown to be feasible by the preceding simulations.

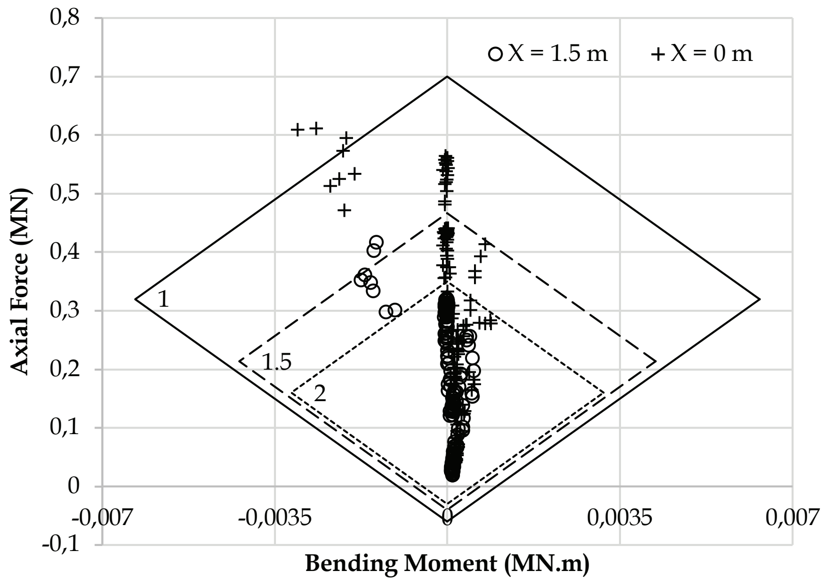

Figure 6. Combined support capacity diagram for X = 1.5 m and X= 0 m 12 hours after installation

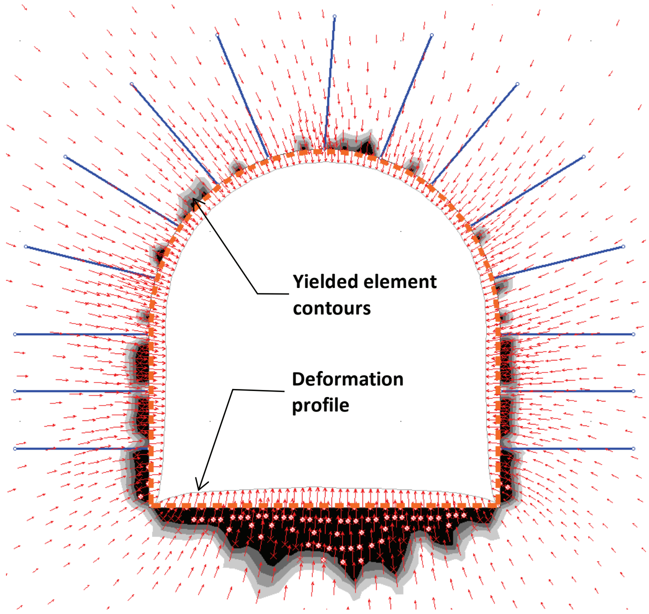

Figure 7. Yielded elements and deformation of final DT2 profile 28 days after support installation

Rock support in tunnel excavations was designed as double corrosion protected permanent support to ensure an adequate level of corrosion protection and long-term functionality of all installed support.

Routine geological mapping during tunnelling was specified following each blast round to confirm the ground conditions encountered and assumptions made during construction, and importantly, identify any ground features which would require a change to the ground support method or notable structurally controlled instability. Such mapping would be augmented by ongoing convergence monitoring to confirm assumptions made during the design of tunnel rock support. These measures combined with controlled perimeter blasting and specified maximum round lengths were adopted to mitigate the risk of structurally-controlled instability.

CONCLUSION

A summary of the methodology used to design the Polihali diversion tunnels has been presented to demonstrate the benefit of a holistic design approach which considers structural instability followed by evaluation of rock support using empirical, convergence-confinement and computational modelling techniques.

This study concluded that the use of conventional drill-and-blast excavation techniques and the installation of rock support comprising rockbolts, welded mesh and shotcrete to within a short distance from the tunnel face, for the construction of the Polihali diversion tunnels, were feasible. Measures identified to mitigate structurally controlled instability associated with sub-horizontal basalt flows included, inter alia, controlled perimeter blasting, routine geological mapping and installation of appropriate levels of rock support. Convergence monitoring was specified to verify assumptions made during the design phase. A minimum shotcrete thickness of 50 mm was specified to seal the rock mass after excavation, and hence mitigate the risk of long-term basalt deterioration.

ACKNOWLEDGEMENTS

The authors wish to acknowledge the Lesotho Highlands Development Authority (LHDA) and thank them for their permission to publish this case study.

REFERENCES

Barton, N. (2002). *Some New Q-value Correlations to Assist in Site Characterisation and Tunnel Design*, Vol. 39, pp. 85–216.

Barton, N. and Grimstad, E. (1993). *Updating of the Q-System for NMT*. Fagernes, Norway.

Barton, N., Lien, R. and Lunde, J. (1974). *Engineering Classification of Rock Masses for the Design of Tunnel Support*, Rock Mechanics, 6(4), pp. 189–236.

British Tunnelling Society (BTS) & Institution of Civil Engineers (ICE) (2000). *Specifications for Tunnelling*.

CEB-FIP Model Code (1990). *Design Code - Comite Euro-Internationa du Beton*, London: Thomas Telford.

Curran, J. H., Hammah, R. E. and Yacoub, T. E. (2002).*A Two-dimensional Approach for Designing Tunnel Support in Weak Rock*.

Hoek, E. (1998). *Tunnel Support in Weak Rock*, in Symposium of Sedimentary Rock Engineering, Taipei.

Hoek, E., Carranza-Torres, C., Diederichs, M. S. and Corkum, B. (2008). 'Integration of Geotechnical and Structural Design in Tunneling', in *Kersten Lecture*. Minneapolis.

Hoek, E., Kaiser, P. K. and Bawden, W. F. (1993), *Support of Underground Excavations in Hard Rock*.

International Tunnelling Association (ITA). *Working Group No. 2: Guidelines for Tunnelling Risk Management*.

Palmström, A. (2009). *Combining the RMR, Q, and RMi Classification Systems*.

Schutz, R. (2010). *Numerical Modelling of Shotcrete for Tunnelling*. Imperial College.

South African National Council on Tunnelling (SANCOT) (1992). *Recommendations on Contractual Practices for Underground Construction*.

Stacey, T. R. & Page, C. H. (1986). Prac*tical Handbook for Underground Rock Mechanics*. Trans Tech Publications.

USACE (1999). *Tunnels and Shafts in Rock*. Washington.

Vlachopoulos, N. & Diederichs, M. S. (2009) *Improved Longitudinal Displacement Profiles for Convergence Confinement Analysis of Deep Tunnels*, Rock Mechanics and Rock Engineering, Vol. 42, pp. 131–146.

Charles Warren-Codrington

Geotechnical Engineer
SMEC South Africa (Pty) Ltd

Charles Warren-Codrington is a professional Civil Engineer who has specialised in geotechnical engineering. He has gained experience in multiple facets of geotechnics, including: the planning and execution of geotechnical investigations, the design and construction monitoring of foundations and ground improvement measures with emphasis on bridge structures, design and construction monitoring of mechanically stabilised earth and lateral support, tunnel rock support and lining design for water conveying and transport tunnels, tunnel operation and maintenance studies and numerical modelling of soil-structure and rock-support interaction. He holds a BSc Eng (Civil Engineering) and MSc Eng (specialised in Geotechnical and Structural Engineering) from the University of Cape Town. He is currently based at SMEC South Africa's Cape Town office.

The effects on the performance of a cable anchor when tensioned by applying torque

J. Greyvensteyn

New Concept Mining, South Africa

The mechanical properties of cables used in underground support are typically attained from pure axial tension tests. A method used to preload support anchors is to apply a tension to a threaded section attached to the cable using a nut. This induces torque which is transferred to the cable which can induce additional stresses. This paper aims to quantify the effect on a cable's mechanical properties after a torque is applied.

For this research, cables were pretensioned using torque applied to a nut located on threaded lengths on the cables. The scope includes both tensioning into the lay of a cable as well as against the lay. The cable is then tensioned further under pure tension until the ultimate tensile strength (UTS) is reached and the cable snaps. The conclusion reached in the paper is that the UTS of the cable is unaffected by the amount of torque applied in the tests, but that the cables behave significantly differently during pre-tensioning

INTRODUCTION

Cable anchors are used throughout the world as a means of mining support. Barrel and wedge axial hydraulic tensioners are commonly used for the pre-tensioning of cable anchors. An alternative method of pretension is to apply a torque to a nut on a threaded section that then tensions the cable. Tensioning via a nut allows for easier mechanisation with standard equipment.

Standard practice is to determine cable mechanical properties in pure axial tension. It is possible that by applying a torque to a cable affects the mechanical properties due to additional stresses induced from twisting the cable. It is therefore important to understand what effects may arise when applying a torque to a cable to ensure that the cable performs as expected.

The aim of this paper is to investigate the effects, if any, on a cable's mechanical properties from applying a torque. The direction of the torque is also considered, relative to the lay of the cable.

Samples

Twelve Ø18 mm compact strand cables were sourced from a single supplier and a threaded component was attached to each end of the cable by means of swaging. A full-length photograph of a swaged stud can be seen in Figure 2. The threads were rolled onto the stud. The total length of the cable was 2.4 m and the free length of cable between the swaging was 1.6 m. The cable had a rated UTS of 380 kN. Six samples were left-hand lay (LHL), and 6 samples were right-hand lay (RHL). The lay of the cable refers to the direction that the individual strands are wound around each other.

Figure 1. Left-hand lay and right-hand lay cable

The twelve samples were split into four groups. The first group comprised of a control group where no torque was applied, the second group comprised of samples where the torque was applied into the lay of the cable, the third group comprised of samples where the torque was applied with the lay of the cable, while the final group comprised of samples where the torque was prevented from passing into the cable but still allowed for the axial movement caused by rotating the nut. The sample layout is demonstrated in Table I.

Table I. The lay of the cable

Group	Sample #	Lay direction	Torque direction relative to lay
1	1	LHL	No torque applied
	2	RHL	
	3	RHL	
2	4	LHL	Into the lay
	5	LHL	
	6	LHL	
3	7	RHL	With the lay
	8	RHL	
	9	RHL	
4	10	LHL	Irrelevant
	11	LHL	
	12	RHL	

Test methodology

During the testing, it was important to ensure that the way in which the cable is gripped did not affect the cable's properties. Barrel and wedge type clamping could not be used as this can affect the strength of the cable due to stress concentrations induced by the internal grooving. American Society for Testing and Materials (ASTM) 370 (Standard Test Methods and Definitions for Mechanical Testing of Steel Products) and ASTM 432 (Standard Specification for Roof and Rock Bolts and Accessories) sets out a standardised testing methodology for cables. However, this is for pure axial tensioning without torque. Although the testing could not conform to the ASTM specifications, the reasoning behind the ASTM specification in not creating stress concentrations was used in selecting how to grip the cable during testing.

Swaged studs were used to connect threaded lengths of steel rod to each end of the cables. The metal studs comprised of a hollow barrel and a male threaded section. The cables were passed into the metal barrel and the outside of the barrel was compressed inwards. This swaged the barrel onto the cable, providing a connection capable of withstanding the axial tension, as well as the torque applied, without inducing a stress concentration in the cable. The swaged studs are demonstrated in Figure 2.

Figure 2. Swaged stud to attach the thread to the cable

An installation machine that allows for the clamping of circular steel tubes on one end while a motor at the other end of the machine applies up to 370 Nm of torque was used to apply a torque to the nut.

To install and pre-tension the cables, a thick-walled steel tube suitable to withstand the expected load of 400 kN was clamped in the jaws of the installation machine. The test cable was located in the tube so that the distal end could not move axially or twist relative to the tube.

Additionally, a ram capable of exerting a load of 520 kN was attached to the proximal end of the tube. Pressurising the ram applied a tensile load to the cable until it reached its UTS and snapped. A typical test setup is demonstrated in Figure 3.

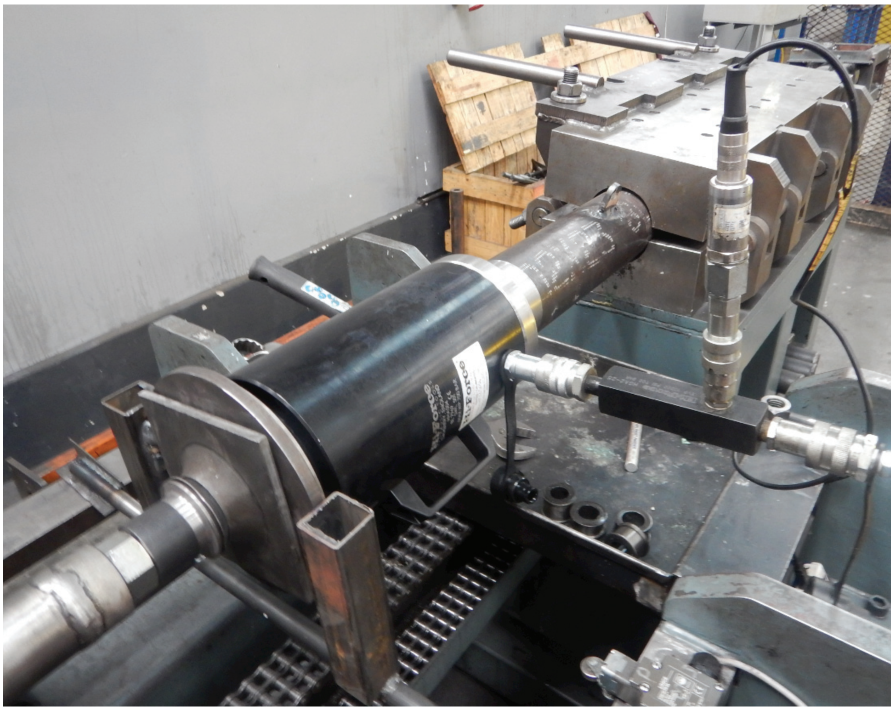

Figure 3. Typical setup of a test

Each test sample was first loaded into the machine and a baseline measurement of the length of stud protruding behind the nut was taken. The sample was then tensioned by applying a torque of 370 Nm to the nut on the cable. Since the ram was positioned between the tensioning nut of the cable and the steel tube in which the cable was installed, an increase in tension within the cable increased the pressure in the ram. Using the effective area of the cylinder and the pressure recorded, the tensile force in the cable could be calculated; the ram therefore acted as a loadcell for the system. Thereafter the installation machine was removed and a second measurement of thread protrusion taken to measure the relationship between exposed thread length and applied torque. The ram was then manually pressurised until cable failure.

For each cable grouping, a representative curve was selected that best demonstrates the characteristic of that group. No mathematical functions were used in the selection of the characteristic curve; the selection of this curve was based on identified trends within the group or the exclusion of curves that exhibited anomalies relative to the other cables in the group. Once a characteristic curve is selected for each grouping, all the group's characteristic curves were plotted on a single graph to determine how the cable behaves under different loading conditions.

RESULTS

Table II shows the loads at which the cables failed, as well as the pre-tensioning thread length measurements for groups 2, 3 and 4. It is noted that the cables, with the exception of sample 11, all failed at a higher tonnage than the rated breaking load of the cable. A component slipped on the sample during tensioning of sample 11, which resulted in the test being abandoned. It appears that applying a torque to an Ø18 mm compact strand cable does not affect the UTS of the cable.

Table II. UTS and thread consumption results

Group	Sample	Breaking load [kN]	Protruding thread before tensioning [mm]	Protruding thread post tensioning [mm]	Thread required to tension with 370 Nm [mm]	Average thread required [mm]
1	1	398	NA	NA	NA	NA
	2	408	NA	NA	NA	
	3	401	NA	NA	NA	
2	4	400	8.15	21.34	13.19	13.9
	5	406	12.55	27.39	14.84	
	6	398	6.92	20.59	13.67	
3	7	408	10.07	15.5	5.43	4.1
	8	401	13.67	18	4.33	
	9	412	12.36	15.03	2.67	
4	10	392	13.7	21.89	8.19	8.1
	11	376	19.35	26.44	7.09	
	12	399	13.16	22.23	9.07	

If the amount of thread required to tension to 370 Nm from group 4 is taken as a reference, half the amount of thread is required when tensioning with the lay (i.e. same direction as the lay) of the cable (group 3). The results suggest that when tensioning with the lay, the cable twists tighter and becomes shorter; this helps to achieve clamping faster. The opposite occurs when tensioning into the lay, i.e. in the opposite direction to the lay (group 2); the cable will open up and become slightly longer, requiring a longer portion of thread for the same amount of torque.

In mining applications, cables are typically used in long lengths. From the results it is apparent that tensioning into the lay requires 3.4 times more threaded length to tension, than if tensioning with the lay. Optimising the direction of tensioning to the lay of steel cables will reduce the length of tensioning required, reducing tensioning times and the length of cable which is left protruding which will in turn maximise the effective length of cable in the support hole.

Group 1 graphs

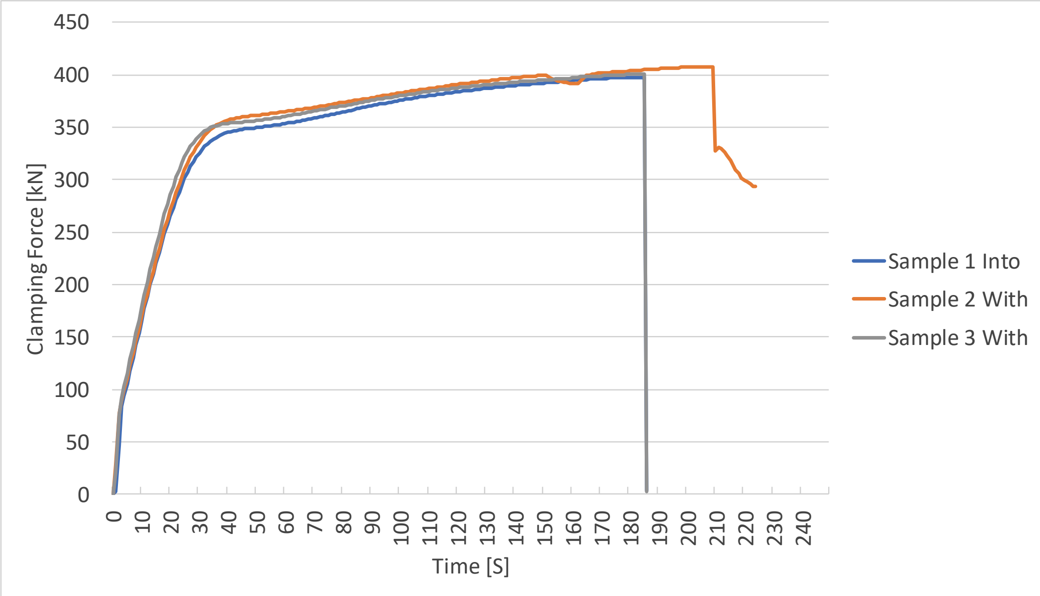

Figure 4. Clamping force of Group 1 cables

Sample 2 failed in an unusual way, as only two of the strands failed. Therefore, sample 2 is excluded as having an anomaly. Sample 1 and sample 3 are both representative of the group, so either can be selected. Sample 1 is selected as the characteristic curve for group 1.

Group 2 graphs

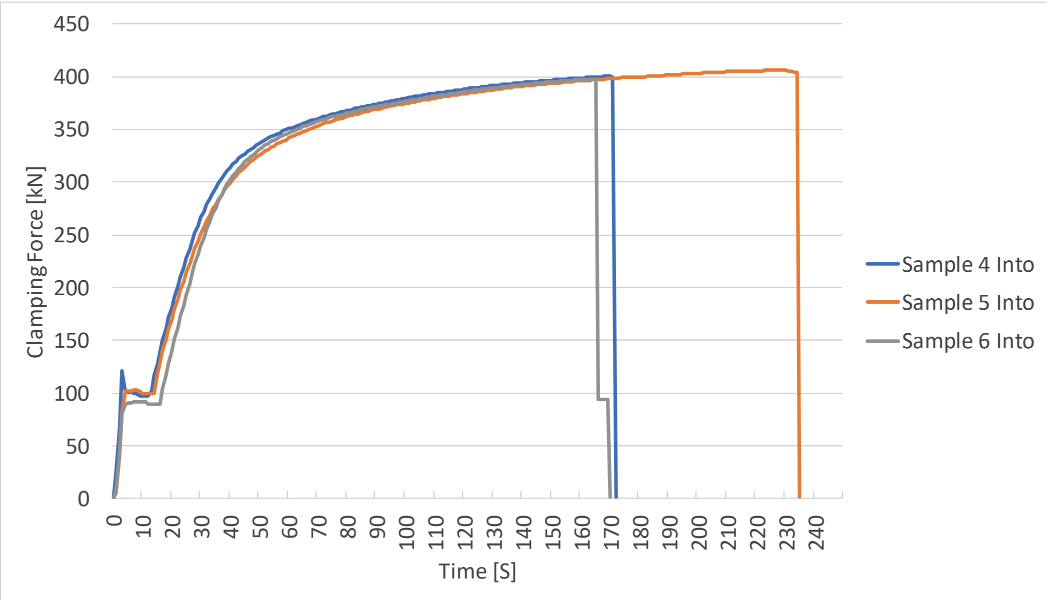

Figure 5. Clamping force of Group 2 cables

Sample 4 is excluded as the characteristic curve as it had an unusual spike in load, then loss of load after pre-tensioning that was not exhibited by the other two graphs within the group. Sample 6 is excluded as its preload was lower than the other two samples. Therefore, sample 5 is selected as the characteristic curve for group 2.

Group 3 graphs

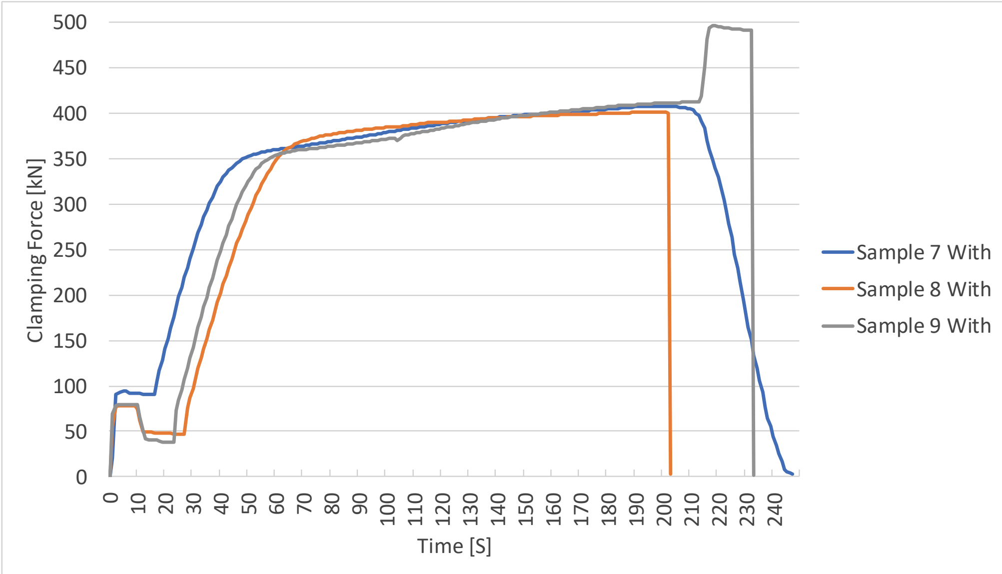

Figure 6. Clamping force of Group 3 cables

Sample 7 is excluded as a cylinder seal failed during the test, causing the cylinder to lose pressure and the clamping force to decrease, also the other two samples showed a decrease in preload when the torque is removed. Sample 9 is excluded as it ran out of stroke on the cylinder before it was able to snap the cable. The spike in load to the end was not experienced by the cable, but was caused by the pressure building to maximum as the cylinder reached maximum stroke. Therefore, sample 8 was selected as the characteristic curve.

Group 4 graphs

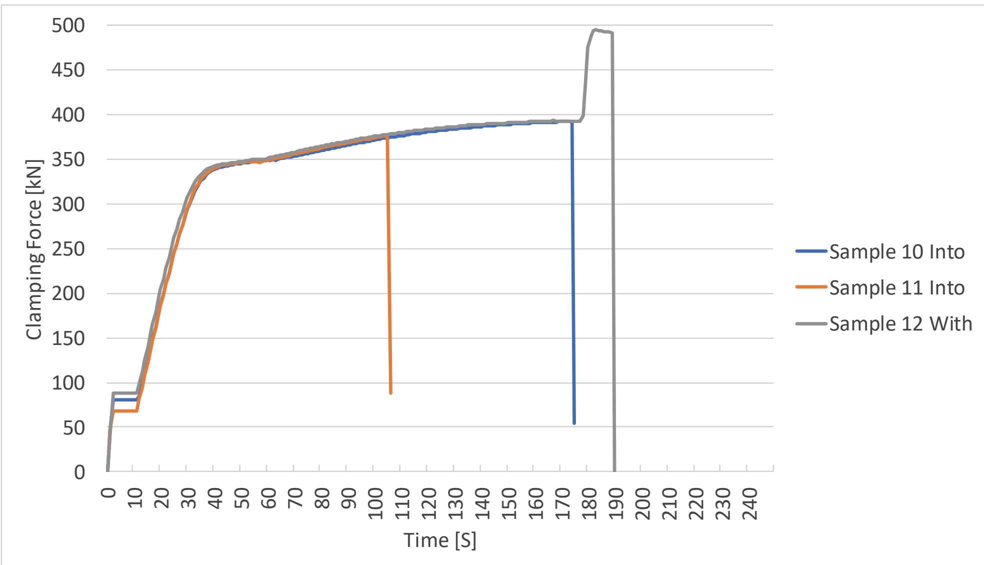

Figure 7. Clamping force of Group 4 cables

As mentioned earlier, a component slipped in sample 11 and the test was aborted and so was excluded. The cylinder ran out of stroke in sample 12 and so it too was excluded. Sample 10 was selected as the characteristic curve for group 4.

Comparison of groups

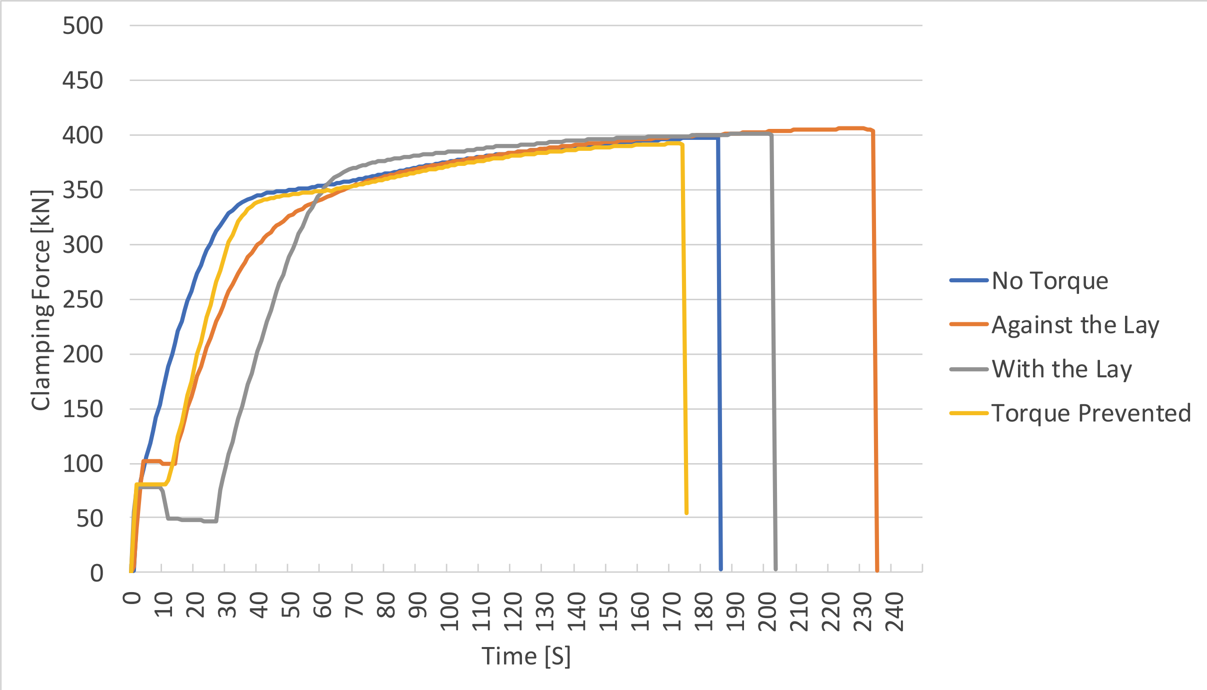

Figure 8. Comparison of characteristic curves

As previously stated, applying torque to a Ø18 mm compact strand cable does not affect its UTS, however, it is interesting to note what occurs after the torque is applied. Tensioning into the lay of the cable produces the highest initial clamping force (pre-tension). Applying torque into the direction of the lay of the cable causes it to open up slightly and therefore lengthen. When the torque is removed, the cable tends to close up again, causing it to shorten slightly, resulting in a slight increase in the clamping force. The opposite is true for tensioning with the lay: the cable winds itself tighter causing the length to shorten. When the torque is removed, the cable tends to return to its normal state. The friction preventing the nut from turning backwards is not high enough and the nut turns backward, releasing tension and causing the clamping force to decrease. When torque is prevented from entering the cable, the cable does not open up or close in and once the torque is removed, the clamping force is stable.

CONCLUSION

This information is pertinent in providing a better understanding of the behaviour of cable support. For example; when very long cable is used, tensioning with the lay of the cable reduces the amount of thread required. However, when the torque is removed, the preload is lost. This is not a desirable situation as the majority of support products have collapsible components to indicate correct preload. During tensioning, the indicator can collapse, but when the torque is removed, the preload drops. Thus, a false positive is witnessed. It is also worth noting that the final pretension achieved is 30% – 50% lower for a given torque than when tensioning into the lay or with zero rotation of the cable.

Should a reliable measure of preload be required, then preventing the torque from transferring into the cable, or tensioning into the lay of the cable is required. Tensioning into the lay results in the highest preload, however, it requires much more thread to achieve the preload. Tensioning while preventing torque from being transferred to the cable, is a suitable compromise between reliable preload and thread requirements.

It should be noted that this paper only considers the effect of torque on the cable. Should the system have an end anchor, then the end anchor must also be able to withstand the torque. If the cable is grouted before tensioning, there is a risk of debonding the grout when a torque is applied that is transferred to the cable.

In conclusion, applying a torque of up to 370 Nm to a nut connected to a Ø18 mm compact strand cable, does not reduce the UTS of the cable. However, the application of torque does have an influence on other properties of the cable, specifically in the pretension phase. These conclusions were based on a small sample size. Trends were witnessed in the pretension phase that justify further testing with a larger sample size to confirm the findings.